Published in final edited form as:
Proc IEEE Inst Electr Electron Eng. 2004 January 1; 92(1): 22–42. doi:10.1109/JPROC.2003.820535.

Dielectrophoresis-Based Sample Handling in General-Purpose Programmable Diagnostic Instruments

Peter R. C. Gascoyne [Member, IEEE] and **Jody V. Vykoukal**
Department of Molecular Pathology, M.D., Anderson Cancer Center, University of Texas, Houston, TX 77030 USA

Peter R. C. Gascoyne: peter@mdanderson.org; Jody V. Vykoukal: jody@mdanderson.org

Abstract

As the molecular origins of disease are better understood, the need for affordable, rapid, and automated technologies that enable microscale molecular diagnostics has become apparent. Widespread use of microsystems that perform sample preparation and molecular analysis could ensure that the benefits of new biomedical discoveries are realized by a maximum number of people, even those in environments lacking any infrastructure. While progress has been made in developing miniaturized diagnostic systems, samples are generally processed off-device using labor-intensive and time-consuming traditional sample preparation methods. We present the concept of an integrated programmable general-purpose sample analysis processor (GSAP) architecture where raw samples are routed to separation and analysis functional blocks contained within a single device. Several dielectrophoresis-based methods that could serve as the foundation for building GSAP functional blocks are reviewed including methods for cell and particle sorting, cell focusing, cell ac impedance analysis, cell lysis, and the manipulation of molecules and reagent droplets.

Keywords

Cell separation; dielectrophoresis; molecular diagnostics; sample preparation

I. INTRODUCTION

Recent progress in the fields of genomics and proteomics has accelerated the identification of genes and gene products that cause or influence numerous disease states. This increasingly molecular understanding of disease necessitates the development of novel technologies that will allow more rapid and facile molecular diagnostics, thereby enabling the benefit of this new information to be realized by a maximum number of people. Additionally, a broad range of potential molecular analysis applications exists in environmental monitoring, agriculture and aquiculture, biotechnology, food production, and public health and safety. When these are taken into account, the scale of future molecular testing needs is staggering, perhaps reaching 15 billion or more tests per year globally in the next ten years. To address such requirements, the current trend of making a specialized disposable device for each test in every application must yield to a more general approach where devices have capabilities suited to multiple molecular analysis needs. Furthermore, for many applications the devices must be capable of parallel, or even continuous, measurements. Inexpensive, miniaturized, and automated devices for general molecular screening will revolutionize the diagnosis and prognosis of diseases and disease risks—even at points of care, in the home, and in environments lacking any infrastructure. Although gene chips and other microscale molecular analysis devices are entering widespread research use today, these cannot address the more generalized needs. They are labor intensive and require sample preparation in a laboratory environment, making them

unsuitable for automatic or continuous monitoring, point-of-care use, or field applications. Skilled technicians are needed to collect and prepare samples through time-consuming, expensive, and heavily infrastructure-dependent techniques. It has been estimated that 90% of the cost and 95% of the time needed to obtain molecular diagnostic data today is associated with sample collection, transportation, and preparation. The inability to effectively prepare samples is perhaps *the* major shortcoming in contemporary molecular analysis systems. This paper considers the application of various ac electrokinetic technologies to this sample handling problem and addresses the development of general-purpose molecular analysis platforms.

A. General-Purpose Sample Analysis Processors

Sample analysis processors capable of general-purpose molecular analyzes might be thought of as the *biochip* equivalents of microprocessors—devices that can be adapted to a wide range of different applications by using appropriate interfaces and software. Microprocessor architecture typically employs multiple functional blocks that are interconnected within a single device but utilized only as required by each application program. Biochips based on a similar design concept would be adaptable to many applications, and production costs would be greatly reduced by mass producing one design for multiple needs. Furthermore, standardized architectures and common programming languages would make application development rapid, efficient, and inexpensive.

General-purpose sample analysis processors (GSAPs) based on this functional block philosophy can be visualized with the core functional blocks selected to realize any steps that may be required for the biomolecular analysis of raw samples. The common goal of such analyzes is to isolate and quantify defined molecular markers from samples that, in the general case, may be highly complex mixtures of cells, debris, and interfering ions and molecules. Fig. 1 shows the sequence of steps needed to realize a typical molecular analysis. A GSAP should, therefore, include functional blocks capable of implementing each of these steps in ways that are sufficiently flexible to accommodate different analysis problems.

An example application for a GSAP is the detection of rare cancer cells in blood, which normally contains a high concentration (4×10^3/μl) of healthy nucleated cells and an even higher background concentration of red cells (4×10^6/μl), platelets (1.5×10^5/μl), and many free proteins—all suspended in a complex electrolyte. Following isolation from the bulk suspension, the rare cells need to be subjected to surface marker and genetic analysis. In this example, the first step in the GSAP would be filtering out and concentrating the small fraction (<0.001%) of morphologically abnormal cells, including those that are putatively cancerous and discarding the remaining blood cells, platelets, and the protein fraction. After this rough separation step has collected a first-cut of the larger cells, further fractionation is needed to discriminate the suspect cancer cells from normal cells. The cancer cells might need to be fractionated from not too dissimilar epithelial or other large cells that may have been cotrapped in the rough separation step. Any residual blood cells and proteins would also be eliminated in this second, more refined fractionation step. Finally, the remaining, putatively cancerous cells would need to be isolated. Cell surface markers such as receptor sites or cluster of differentiation (CD) antigens could be labeled during this isolation step. However, important gene and protein markers are inside the target cells. Cell lysis is required to liberate these molecular targets. Lysis releases a mixture of molecules, including nucleases and proteases which have the unfortunate tendency to destroy the molecular markers we hope to detect. Other entities, especially trace metal ions, can potentially interfere with molecular assays. It is, therefore, necessary to capture the released target molecules, remove possible interferents and incubate the target molecules with nuclease- and protease-inhibitors. Only after these cell fractionation and molecular isolation steps are completed do we arrive at the molecular

detection and measurement steps that are the main focus of current efforts to produce gene chip and microfluidic analysis devices.

A programmable GSAP device capable of accomplishing the sample preparation and analysis steps shown in Fig. 1 would function in a diverse range of applications. Potential uses include the identification and quantification of diseased cells in humans and animals, bacteria or viruses in blood and urine, bacteria or fungi in foodstuffs and drinking water, microbes in wastewater, as well as target agents in the environment, in the body, and in industrial processes. By programming a general-purpose device to execute or bypass various sample preparation and analysis steps as appropriate, a single biochip design could satisfy the processing needs for these and other applications. Thus, if the cells emerging from the first two separation steps had unique and readily identifiable molecular markers on their surfaces, the intracellular molecules would not need to be assayed. The cells could be labeled at the isolation stage and measured at the analysis stage without undergoing cell lysis or molecular capture: the GSAP would simply be programmed to allow the sample to flow through unnecessary stages without processing. Similarly, if free biomolecules were to be subjected to analysis, samples would flow unprocessed though the cell sorting and isolation stages directly to the molecular quantification step.

Fully three-quarters of the steps in Fig. 1 are different forms of sample preparation and handling —only one quarter comprise the actual molecular measurements. Although these molecular analysis steps are the central function of a microfluidic diagnostic device, they have not proven to be the most challenging aspect in realizing such devices. Most current molecular methods [e.g., polymerase chain reaction (PCR) and nucleic acid or antibody labeling] are adapted from biological processes that are native to living cells having volumes in the femtoliter range. If anything, reducing the assay scale from existing benchtop machines to microfluidic devices brings the biochemistries closer to the scale on which they evolved. By contrast, sample preparation methods are generally unprecedented in nature. Current bench-based biosample preparation methods do not necessarily scale well to the microfluidic domain where less familiar physical phenomena (e.g., capillary forces and laminar flow) become dominant. While valves are straightforward to realize in bench-scale systems, it is very difficult to make them reliable and leak- and fouling-free at the micro- and nanoscales because of the much larger influence of viscous and capillary forces acting at this scale. Mixing is also problematic, and ubiquitous benchtop methods such as centrifugation are cumbersome to implement on the microscale. On the other hand, physical effects that may be of limited or no use in macrofluidic devices may become useful on the microscale and offer unanticipated new opportunities for sample handling. Additionally, small-scale effects such as rapid heat dissipation and high power density can be used to an advantage in microfluidic diagnostic devices. Thus, capillary electrophoresis provides superb molecular discrimination, microscale PCR cycling times can be on the order of seconds, and generally unexplored physical phenomenon such as dielectrophoresis (DEP) can be used to move and discriminate matter. If the goal is to build small, self-contained, efficient microsystems, the best approach is to rethink the old concepts of sample preparation and measurement methods in the light of microscale physics. One useful change in thinking is in defining what constitutes a sample. On the benchtop, a *sample* usually means a volume of liquid that contains the materials to be assayed, and moving a sample means transporting this liquid. In microsystems, where distances are small and forces can be used to move the materials of interest *within* their supporting liquid, a *sample* can mean the materials of interest viewed independently from their suspending medium. Several phenomena can be used to manipulate particles, cells, and molecules on the microscale including electrophoresis, magnetophoresis, DEP, and acoustic focusing. In principle, any type of force that can be applied to particles, cells, and molecules (including, for example, gravity, acoustical, thermal, electric, and magnetic) could be used in microsystems for sample manipulation. From a practical standpoint, however, a general purpose device would be most versatile if the force field is

applicable to every sample type and is easy to control. It will be seen later that ac electrokinetic methods are quite generally applicable and adaptable to a broad range of different sample types. Furthermore, they are easier to implement, reconfigure, and control than other manipulation methods. For these reasons, ac electrokinetic methodology will form the focus of this chapter although it is recognized that other sample preparation methods may need to be employed in specific GSAP applications.

II. DEP

If a particle is placed in an inhomogeneous electric field, it will, in general, experience a translational force [1]–[3]

$$\overline{F}_{\text{elec}} = q\overline{E} + (\overline{m} \cdot \nabla)\overline{E} + \frac{1}{6}\nabla(\overline{Q} : \nabla\overline{E}) + \cdots. \tag{1}$$

Here, $q\bar{E}$ is the well-known coulombic force due to the net charge q of the particle and the electric field $\bar{E}$. This embodies all aspects of electrophoresis and vanishes in an alternating electric field or the absence of a net charge on the particle. The additional terms to the right of the electrophoretic force arise from the interaction of dielectric polarization in the particle induced by the electric field with spatial inhomogeneities in that field. Here, $\bar{m}$ is the dipole moment induced by the field, and $\vec{Q}$ is the quadrapole tensor induced by the applied field. The polarization forces vanish only if the electric field is spatially homogeneous or if the particle has dielectric properties that are identical to its surroundings. Pohl [4] referred to the migration of particles caused by electric dipole forces [the second term in (1)] as *"dielectrophoresis"* but here we use "dielectrophoresis" to mean all force components embodied in (1) associated with inhomogeneous fields, including quadrupole ($\vec{Q}$) and higher order dielectric phenomena as well as traveling wave effects that arise from time-dependence of the electric field distribution.

A. Dielectrophoretic Theory

If the time-averaged DEP force on a particle resulting from an ac electric field, $\bar{E}(\omega)$, is approximated as the dipole polarization force, it can be written as

$$\left\langle \overline{F}(t) \right\rangle = 2\pi\varepsilon_m r^3 \{\text{Re}(f_{\text{CM}}(\omega))\nabla E_{\text{RMS}}^2 + \text{Im}(f_{\text{CM}}(\omega))\,(E_x^2\nabla\varphi_x + E_y^2\nabla\varphi_y + E_z^2\nabla\varphi_z)\}. \tag{2}$$

Here f_{CM} is the Clausius–Mossotti factor which describes the frequency-dependent dielectric characteristics of the particle and its surroundings that account for the induced dipole moment $\bar{m}$ in (1). r is the particle radius, ω is the angular frequency, and E_{RMS} is the root-mean-square (RMS) value of the applied electric field. E_i and $\varphi_i (i = x, y, z)$ are the magnitudes and phases of the electric field components along the principal axes. In this approximation the quadrupole and higher terms of (1) are assumed to be zero. This is often, but not always, the case for slightly to moderately inhomogeneous electric fields. We and others [1]–[3] have derived force equations that include higher order terms and a of situations where these may need to be considered [2], [5].

Equation (2) shows there are two independent terms contributing to the DEP force.

1. The first is a force proportional to $Re(f_{\text{CM}})$, the *real* (in-phase, or capacitative) component of the electrical polarization induced in the particle, and to the spatial nonuniformity of the electric field, ∇E_{RMS}^2. This force causes particles to move toward strong or weak field regions in accordance with whether $Re(f_{\text{CM}})$ is positive or

negative, reflecting whether the particles polarize more or less than their suspending medium in the applied field. It allows particles to be attracted to or repelled from electrode edges, for example. This is the force originally identified by Pohl [4] as dielectropheresis, but as already indicated we use the term more generally here.

2. The second is a force proportional to $Im(f_{CM})$, the *imaginary* (out-of-phase, or lossy) component of the particle polarization, and to the speed with which the electric field distribution is traveling as reflected by the electric field phase gradients $\nabla\varphi_x$, $\nabla\varphi_y$ and $\nabla\varphi_z$. This force causes particles to move with or against the direction of field travel depending upon whether $Im(f_{CM})$ is positive or negative, i.e., whether the particles are more or less electrically lossy than their surroundings. It allows particles to be moved parallel to and across electrodes. At least three electric field excitation phases must be provided to an electrode array for this force to arise because this is the minimum configuration for creating an electric field distribution that moves through space.

B. Versatility of DEP Forces

Because the two DEP force components act independently they can be exploited alone or in combination by applying appropriate electrical signals to electrode arrays designed to create the required electric conditions. It is illustrative to recognize the relationship between dielectrophoretic forces and optical forces applied by laser tweezers [6], [7]. Although DEP typically uses electric fields with wavelengths that are significantly larger than the particle diameter and optical tweezers use wavelengths of the same order of size as the particle, both methods depend on the electric field energy gradient and on the differences between the electrical permittivities and loss (or the corresponding refractive indices and dispersions) of the particle and its surroundings. Yet while optical tweezers must drag particles around using tightly focused beams of light as “tractors” generated by optical components that are inherently narrow band, the near field characteristics of DEP means that fields can be generated by an array of “microscopic antennae” patterned to allow particles to be manipulated *anywhere* inside a device simply by switching electrical signals that may span six or more decades in frequency.

Just as the refractive index and dispersive properties at infrared (IR) and optical frequencies are wavelength dependent, the dielectric properties of particles, as embodied in f_{CM}, are frequency dependent. The inherent versatility of DEP can be exploited by using a field whose frequency can be adjusted to optimize each application in accordance to the dielectric characteristics of the particles undergoing manipulation and discrimination. The dielectric properties of a particle typically reflect several aspects of its structure and composition—DEP can, therefore, enable enhanced particle discrimination that accesses multiple particle properties. This is in contrast to electrophoresis, in which particle discrimination is entirely dependent upon the ratio of particle charge to hydrodynamic drag. Differences in dielectric properties can be exploited to impose different and even opposing forces on different particle types within a mixture. The defining nature of DEP is the movement of objects with respect to a suspending medium in which an inhomogeneous field is present. Particles can be concentrated to a focal point by negative DEP or trapped by positive DEP, and different particle types can be moved apart from one another all under appropriate field conditions. Once a *sample* is understood to mean the analytes *inside* a suspending medium, the versatility of DEP for sample handling becomes apparent. It is fair to say that if appropriate conditions can be imposed, DEP can *move any particle that can be seen* and *separate any two particles that look different*, where it is understood that, in principle at least, the optimal frequency to do the “seeing” may be chosen anywhere in the spectrum from near dc to near IR.

C. Dielectric Properties of Debris, Cells, and Molecules

Equation (2) shows that the properties of a particle that determine its DEP responses are embodied in the Clausius–Mossotti factor f_{CM}, which can be expressed as

$$f_{\mathrm{CM}}(\varepsilon_p^*, \varepsilon_m^*, \omega) = \frac{\varepsilon_p^*(\omega) - \varepsilon_m^*(\omega)}{\varepsilon_p^*(\omega) + 2\varepsilon_m^*(\omega)}. \tag{3}$$

where $\varepsilon_p^*(\omega)$ and $\varepsilon_m^*(\omega)$ are the complex permittivities of the particle and the medium, respectively. Each complex permittivity takes the form $\varepsilon^* = \varepsilon - j(\sigma/\omega)$, where $j = \sqrt{-1}$, and the dielectric constant of the material is ε and its electrical conductivity is σ. Because particle electrical polarization is not instantaneous, complex permittivities of the particle and medium depend on the frequency $f = \omega/2\pi$ of the electric field.

While the components of ε_m^* for a homogeneous medium are simply the bulk permittivity and conductivity, the components for particles are more complicated because all mechanisms of polarization [8] and electrical conductivity within all components of their structure may contribute, including those of the boundary layer between the particle surface and the suspending medium. From the dielectric standpoint, an extremely fortunate characteristic of many biological entities is that they are encapsulated by some form of envelope. Thus all viruses, phages, and prokaryotic and eukaryotic cells comprise protein coats or membranes which interface them to the outside world and confine one or more regions that contain aqueous electrolytes that support the activities of life. Ions in the aqueous phases inside and outside a cell tend to move under the influence of an electric field until they encounter an obstruction. A build up of ions at cellular membranes results in so-called interfacial polarization—this process dominates the dielectric properties of living things at frequencies up to 200 MHz, swamping smaller contributions from electronic and fixed dipolar polarization processes. Thus, in the frequency range 5 kHz–200 MHz, the dielectric properties of cells are dominated by polarization at membrane interfaces governed by cell membrane morphologies, internal conductivities, and compartment size [9]–[15]. Above that frequency dipolar and electronic polarization effects dominate, but these have yet to be exploited seriously for DEP sample preparation and discrimination.

Although both the inside and outside surfaces of a cell membrane exhibit interfacial polarization, if the conductivity of the electrolyte outside a cell differs from that within, the characteristic times for polarizing the inside and outside surfaces of the membrane will differ. This condition can be ensured by suspending cells in a medium having a lower conductivity than the cell interior (usually by a factor of at least two and preferably more). Under these conditions, a cell has a distinct *dielectric signature* that makes its discrimination from background particles straightforward by ac electrokinetic methods. Furthermore, this approach emphasizes the dielectric differences between different cell types and enables one type to be discriminated from another.

To understand the dielectric properties of different particle types that may be present in a sample, it is helpful to use dielectric models. Just as a complex network of resistors and capacitors may be modeled as an equivalent circuit that is usually more simple, so the complex dielectric properties of a structure may be represented by an equivalent dielectric shell model [16]. The shells in the model need not have a one-to-one correspondence to physical structures in the real particle. However, in an effort to understand and quantify the physical processes at work, it is usual to choose a model that approximates the particle structure as far as practicable. We have shown that if the dielectric model has the same structure as the real particle, then the parameters deduced from experimentally measured dielectric responses approximate the true

physical properties of that particle [17]. Generally, such approximations are reasonably accurate; however, under certain circumstances, this may not be the case [18]. Fig. 2 shows dielectric shell models for point particles, solid particles, particles with a single compartment surrounded by a thin envelope, and particles with two concentric compartments surrounded by thin envelopes. These models can be used as tools for understanding the dielectric properties of molecules, inert particles, entities with a single membrane (such as viruses, prokaryotes, and eukaryotes having small nucleii), and more complex cells (such as plant cells or mammalian cells with large nucleii), respectively. The models include permittivity and conductivity parameters for the suspending medium, for all of the shells that make up the cell, and for an extra shell corresponding to the interface between the particle and the medium. This extra shell owes its existence to fixed charges on the particle. Although DEP employs ac electric fields for which electrophoresis effects are zero, fixed charges on the particle induce a charge double layer within the suspending medium in which the ionic concentration may be altered by orders of magnitude compared with the bulk suspending medium. This region has its own dielectric properties that contribute to the overall ac electrokinetic forces [19]–[22] experienced by the particle.

Simulated dielectrophoretic response spectra are shown beside each particle type in Fig. 2 (the exact spectral responses vary according to particle dimensions and shell compositions). Each spectrum shows that the frequency of the applied electric field is a critical determinant of the particle ac electrokinetic response, and each is a signature for the particle type. Each frequency dependency results from the time required for the various electrical polarizations to build up in various structures of the particle and this lends a dimension of discrimination to DEP that is absent from electrophoresis. It is evident from Fig. 2 that cellular structures, with their encapsulating membranes, have fingerprints that are distinct from structures that lack membrane encapsulation.

The DEP force corresponding to each dielectric shell depends on the volume of that shell. For molecules and very small particles, the volume of the charge double layer region is comparable to or larger than the particle itself, and this region, therefore, is the most important in determining the ac electrokinetic responses. In fact, the DEP responses of molecules are so completely dominated by the charge double layer that discrimination between subtly different molecules is impossible. We will return to this point later when we consider how DEP might be used to provide precise recognition and manipulation of biomolecular targets possessing very small differences. Charge double layer and surface conductivity characteristics lead to useful differences between the dielectric properties of gram-negative and gram-positive bacteria, however [23], [24], and are important considerations in the DEP responses of viruses [25], [26].

Because different cell types are morphologically distinct they have different *dielectric phenotypes* [27] making DEP an attractive method for cell manipulation and discrimination. The frequency spectra of cells can be measured with single-cell discrimination using the method of electrorotation (ROT) in which the rotation of cells resulting from the torque induced by an applied rotating electric field is measured as a function of the field frequency [12], [13], [17], [28]–[42], by computerized analysis of DEP motion [43], or by multifrequency impedance analysis [44]–[46]. For most practical purposes, the dielectric properties of mammalian cells can be adequately described by the single-shell model [16], [17], [47], [48]; the cellular dielectric parameters deduced from analysis of frequency spectra may be used to predict the DEP properties for both inhomogeneous and traveling fields under any given operating conditions, permitting exploration of the optimum conditions for separating dissimilar cell types. Fig. 3 shows ROT spectra and DEP collection spectra for the breast cancer cell line MDA231, normal T-lymphocytes, and erythrocytes. Note that at certain so-called *crossover frequencies* the DEP force traverses zero and its direction reverses. The crossover

frequency, which defines the frequency at which DEP trapping ceases and DEP repulsion will begin, is useful for discussing DEP behavior and it will be used for describing cell separations in this chapter. The DEP crossover frequencies for several mammalian cell types have been experimentally determined and are summarized in Fig. 4. Spectral responses for different bacteria have been given by Markx *et al.* [23].

D. Sample Conditions

Cellular dielectric properties reflect cell structure and the internal and external electrolyte environment. Because the dominant polarization mechanism is interfacial, the configuration of membrane interfaces, and most especially that of the outer membrane, is an important determinant of cellular DEP responses. Indeed, we and others have demonstrated that the dielectric properties of cells most sensitively reflect the structure of their plasma membrane [12], [13], [17], [28], [31], [33], [34], [36], [40], [49]. The cell membrane has four parameters that control its complex permittivity, including the membrane thickness, effective area, dielectric constant, and electrical conductivity. Under conditions used for most DEP manipulations, the plasma membrane conductivity of healthy cells is usually negligible, though this is not true of diseased cells [14], [50]. The dielectric constant remains constant within a few percent even for widely ranging protein/lipid ratios, and membrane thickness can change by perhaps 10% depending on the lipid composition [12], [51]. On the other hand, the effective membrane area, as determined by surface morphology including folding, ruffling, and microvilli, can vary over a 20-fold range for different cell types. Therefore, while the membrane capacitance of a smooth biological membrane is approximately 0.8 μ*F*/cm^2 ± 15%, we have measured cell membrane capacitances ranging from 0.8 μF/cm^2 for smooth cells up to 15 μF/cm ^{2} in the case of highly convoluted hepatocyte membranes. Nevertheless, most mammalian cells have membrane capacitances in the range 1.2 to 4 μF/cm^2.

The morphological properties of mammalian cell membranes sensitively and dynamically reflect the physiological state of the cells. As the interface of cellular signaling and transport events to and from the outside world, the membrane structure is regulated in accordance with the physiological state, metabolism, and environment of the living organism. Growth factor levels, glucose concentration, pH, cell density, and temperature are among the external factors that determine the activities of mammalian cells. As a result, if consistent DEP results are to be obtained from cultured cells, for example, then consistent seeding concentrations, pH buffers, serum lot, and consistent harvest concentrations and methods should be used. The recent advent of proteomic analysis has served to further underscore the importance of such details.

Like mammalian cells, bacteria and other single-cell types show responses to their surroundings and supporting media, though their outer membranes tend to be more stable and hardy than those of cells isolated from native conditions in multicellular organisms. Such responsiveness of cells to their environment might seem like a disadvantage of DEP methods. However, the observed changes in cellular dielectric properties leave basic cellular dielectric fingerprints recognizable, and the sensitivity means that DEP can be used to observe real-time responses to challenges such as stimulation by mitotic [52] and differentiating agents [12], growth factors, drugs, and toxicants [32], [49], [53], [54].

III. CELL AND PARTICLE SORTING

A. DEP Trapping

DEP trapping is useful for concentrating cells from a suspension as demonstrated for yeast, bacteria, mammalian cells, and other cell types [55]–[60]. Once concentrated, the simplest, though least discriminating, method of exploiting dielectric differences for particle separation

is *differential affinity DEP* whereby an ac electric field is used to trap one particle type by positive DEP while simultaneously repelling other types by negative DEP.

In order to bring about separation [56]–[60], the differential DEP forces experienced by the different particle types must be sufficiently great. A separability parameter for two particle types has been defined [27] as

$$S = r_1 \mathrm{Re}(f_{\mathrm{CM1}}) - r_2 \mathrm{Re}(f_{\mathrm{CM2}}) \quad (4)$$

where r_1 and r_2, and f_{CM1} and f_{CM2}, are the radii and Claussius–Mossotti factors, respectively, of the two particle types. If S is small, as is the case for many mammalian cell separation problems, the different cell types will experience weak DEP forces when DEP affinity separation is being attempted, the differential forces driving separation will be very small, and a low separation efficiency will result.

Nevertheless, when particle compositions or cell sizes and morphologies are clearly distinct, good separation efficiency is usually possible by this method. This is the case when DEP is applied to the beneficiation of ores [61] and dewatering of aqueous dispersions of clays [62], the separation of bacteria from mammalian cells [63], of live cells from dead cells [64], and of cells from debris, for example. As a mammalian cell example, we have demonstrated that it is possible to recover 100% of human breast tumor cells from peripheral blood mononuclear cells (PBMNCs) even at the most dilute concentration we have currently tested, one tumor cell per 2×10^6 PBMNCs. In this case, we applied slow fluid flow to a mixture of blood and tumor cells, the blood cells were eluted from the DEP chamber, and tumor cells were recovered by lowering the DEP frequency, causing them to be repelled from the electrodes by negative DEP [65]. Some normal cells were associated with the tumor cells during the trapping phase and while recovery efficiency was extremely good, purity is not always adequate. In general, we have found it impractical to separate cells having less than a 50% difference in their crossover frequencies using DEP differential affinity alone.

At high frequencies (typically 200 kHz or more), all *viable* cells can be trapped by positive DEP regardless of type, if the conductivity of the suspending medium is well below that of the cell interiors. This is readily achieved for viable cells at suspending medium conductivity <400 ms/m, corresponding to a medium containing 25% or less ions than physiological conditions. In the case of mammalian cells, the osmolarity of the suspending medium must be compensated to physiological levels to avoid cell stress or damage. We have typically used suspending media conductivities in the range 10–200 mS/m containing sucrose or mannitol to compensate the osmolarity to 300 mOs/Kg. Under these conditions, DEP can be used quite generally to immobilize cells without regard to cell type for washing or perfusion with reagents and for separation of viable cells from dead cells and debris. In such experiments it is important to include dextrose (for example at a concentration of 2 g/L) as a fuel for metabolic energy for mammalian cells to remain viable. If this is provided and frequency and voltage ranges are kept within nondamaging bounds, cells can be manipulated for 40 min or more and then returned to normal culture without damage. We have described analyzed safe operating conditions elsewhere [66].

Dielectric and hydrodynamic interactions between neighboring trapped cells, differences between DEP forces at different locations of an electrode geometry, and the multivalued solutions of the force balance equation between opposing positive DEP, gravitational, and hydrodynamic lift forces all serve to limit the discrimination of differential affinity DEP sorters [5]. Nevertheless, DEP trapping offers high throughput and good discrimination between viable and nonviable cells and debris. The attainable concentration factor is substantial and provides

a useful first step toward isolating pure target cell subpopulations. Finally, the electric field frequency and voltage used for DEP may be easily programmed to accommodate a wide variety of sample preparation applications with the same electrode configuration. In other words, DEP differential affinity filtering is electrically programmable and may be programmed in a matter of microseconds under electronic control. As an advance on our earlier tumor cell work, an example of an excellent implementation of differential affinity DEP followed by molecular analysis in a microfluidic setting has been demonstrated by Huang *et al.* [67]. Systems for cell and bacterial analysis have also been shown [68], [69].

B. Field-Flow Fractionation

Field-flow fractionation (FFF) is a family of methods in which particles are characteristically positioned within a fluid flow velocity profile by balanced forces [70]. Different particle types are then carried at different characteristic velocities in accordance with their positions in the fluid flow stream. Using this principle, a sample mixture can be introduced at one end of a flow channel and fractionated along the channel as the different constituent particle types are transported at different rates. The different particle types emerge from the other end of the flow channel at different times. Giddings [70] and others [71]–[73] elucidated three primary modes of FFF: *normal, steric*, and *hyperlayer*. Normal FFF, involves thermal diffusion profiles of sub-micrometer-sized particles. As a rough guide, Brownian motion and thermal diffusion are negligible for particles above the order of 1 μm in diameter at room temperature. In steric FFF, the applied force causes the particles to impact one side of the separation chamber, resulting in steric hindrances that characteristically diminish particle velocity in the flow stream. In hyperlayer FFF, particles are characteristically positioned within the flow stream away from the chamber walls and are carried at the velocity of the fluid at that position.

Differential affinity DEP with fluid flow used to elute some particles is an extreme form of steric FFF in which the steric forces act to largely immobilize at least one of the particle species. In this case (see Fig. 5), particle behavior is determined by three main factors—the DEP force, the particle sedimentation force, and the hydrodynamic lift force (HDLF). HDLF occurs whenever particles are placed within a fluid velocity gradient and tends to move the particles away from flow channel walls into the faster flowing region. In microfludic systems using aqueous suspensions, the flow velocity profile $v_p(h)$ is almost perfectly parabolic

$$\upsilon_p(h)=6\langle\upsilon\rangle\frac{h}{H}\left(1-\frac{h}{H}\right) \tag{5}$$

where h is the height above the chamber bottom, $\langle\upsilon\rangle$ is the mean fluid velocity, and H is the chamber height.

When the positive DEP force on particles is sufficiently strong, there is only one equilibrium condition corresponding to particles being trapped on the electrode. At lower positive DEP force levels, however, there is a regime in which particles may have as many as three equilibrium positions in the flow stream [5]. One of these corresponds to DEP trapping, the other two to conditions in which the HDLF and sedimentation forces balance the DEP forces away from the chamber wall. Particles will move at different velocities at these different equilibrium positions, and it follows that differential affinity DEP separation is not uniquely defined, most especially for weak DEP forces inherent in operating at an electric field frequencies close to the DEP-crossover frequency as demanded for only slightly dissimilar cell types.

Because of vibration, uneven fluid flow, and field imperfections, particles experiencing small positive DEP forces can move between equilibrium states and an ill-defined elution profile

with very poor separation will result. This problem can be overcome if particles are always *trapped* from a levitated position in the moving fluid rather than being *released* from a trapped position [5]. Thus, for optimal DEP separation by DEP differential affinity, a particle mixture should not be trapped and then released by increasing the flow rate, lowering the applied voltage, or slowly reducing the field frequency. If sequential release of multiple particle types from a trapped mixture is desired, the entire population of trapped particles should be released after each separation step and then retrapped under the new separation conditions [5].

1) Hyperlayer DEP–FFF—To overcome the disadvantages that limit the discrimination of DEP differential affinity separation, the method of hyperlayer DEP–FFF was developed. Rather than using positive DEP, this technique balances a levitating negative DEP force against a force that directs particles toward the electrode array. In sedimentation DEP–FFF, the levitating effects of negative DEP are balanced against the particle sedimentation force (see Fig. 6). The DEP force falls exponentially with height above the electrode array [74] and particles are carried through the chamber at velocities given by (5) according to their respective equilibrium levitation heights.

These equilibrium heights are given by

$$h_{\mathrm{eq}}=\frac{d}{2\pi}\ln\left\{\frac{3\varepsilon_m E_{\mathrm{RMS}}^2 \mathrm{Ap}}{2(\rho_c-\rho_m)g}\mathrm{Re}(f_{\mathrm{CM}})\right\} \tag{6}$$

where d is the spacing of electrodes in the DEP electrode array, ε_m is the real part of the permittivity of the suspending medium, E_{RMS} is the RMS electric field, the term Ap takes into account any reduction of the field strength experienced by particles due to electrode polarization effects, $(\rho_c - \rho_m)$ is the difference between the density of the particles and their suspending medium, and g is the acceleration of gravity [74], [75]. Levitation heights for DEP–FFF separation of cells can range from almost zero to 60 μm or more. Unlike the equation for differential affinity DEP, (6) is always single valued for negative DEP forces, yielding identical elution times for all particles of the same type. Different particle types maintain their differential velocities as they traverse the separation chamber, leading to a spatial separation that is cumulative—greater separation is obtained for increasing chamber length, L. In contrast, separation by DEP trapping is a single-shot effect tht cannot be improved by altering the chamber geometry.

A particularly useful characteristic of hyperlayer DEP–FFF is that its discriminating power is a function of the levitation height because the flow velocity gradient and DEP force are both height-dependent functions. Since the particle height can be adjusted by altering the DEP frequency and voltage, the discrimination of hyperlayer DEP–FFF can be electrically programmed. When the levitation height h is small compared to the chamber height H, the elution time for a particle can be approximated as

$$T_{\mathrm{elution}}=\frac{2\pi \mathrm{LH}}{6d\langle\upsilon\rangle\left[\ln\left\{\frac{3\varepsilon_m E_{\mathrm{RMS}}^2 \mathrm{Ap}}{2(\rho_p-\rho_m)g}\mathrm{Re}(f_{\mathrm{CM}})\right\}\right]} \tag{7a}$$

At frequencies much lower than the crossover frequency, $Re(f_{\mathrm{CM}}) \rightarrow -(1/2)$, and the elution time depends on particle density, providing a microfluidic sorting method that can function like a centrifuge. At higher frequencies, the particle elution time depends sensitively on the frequency-dependent particle dielectric properties and may be written as

$$\frac{\partial T_{\text{elution}}}{\partial \operatorname{Re}(f_{\text{CM}})} = -\frac{2\pi \text{LH}}{6d\langle v\rangle \operatorname{Re}(f_{\text{CM}}) \left[\ln\left\{\frac{3\varepsilon_m E_{\text{RMS}}^2 \text{Ap}}{2(\rho_p-\rho_m)g}\operatorname{Re}(f_{\text{CM}})\right\}\right]^2}. \tag{7b}$$

As the DEP crossover frequency is approached, $Re(f_{\text{CM}}) \rightarrow 0$, or as the field E_{RMS} is reduced, the DEP levitation force decreases so that $(3\varepsilon_m E_{\text{RMS}}^2 \text{Ap})/(2(\rho_c - \rho_m)g)\text{Re}(f_{\text{CM}}) \rightarrow 1$ and the discriminating power of the separation increases [74], [75]. Although this suggests that the discriminating power may be electrically adjusted toward *infinity*, (7a) and (7b) hold only when the levitation height is predicted to exceed the particle radius $((d/2\pi)\ln\{(3\varepsilon_m E_{\text{RMS}}^2 \text{Ap})/(2(\rho_c - \rho_m)g)\text{Re}(f_{\text{CM}})\} > r_{\text{particle}})$, otherwise particles approach the chamber floor and steric and hydrodynamic lift effects cause the relationship to break down. This steric regime where DEP forces are so weak that they are unable to cause either levitation or trapping corresponds to conventional steric FFF. In this regime, FFF velocities depend sensitively on the particle and chamber surface characteristics and on hydrodynamic lift effects in very close proximity to the wall [70], [71], [72]. It follows that the DEP trapping and hyperlayer DEP–FFF regimes, wherein particle behavior is uniquely determined by the electric field characteristics of the chamber and the dielectric properties of the particles, are separated by a conventional steric FFF regime defined by particle and chamber surface interactions and hydrodynamic lift effects.

If desired, DEP trapping, steric, and hyperlayer DEP–FFF may be used independently, simultaneously, or sequentially in the same chamber to separate complex particle mixtures depending how the electric field is programmed. Thus particles having a low crossover frequency can be trapped while those having higher crossover frequencies may be separated with high discrimination by hyperlayer DEP–FFF at the same time. Later, the field frequency or the solution conductivity may be adjusted to release trapped particles and those can then be subjected to their own high discrimination hyperlayer DEP–FFF separation with different field settings. In this way complex particle mixtures may be fractionated in one or more electronically programmed steps.

A number of groups have successfully applied DEP–FFF to particle fractionation, including the separations of latex microspheres [74], [76], [77], stem cells from tumor cells [78], [79], and blood cell subpopulations [80]. One example that illustrates the ability of the method to discriminate changes as subtle as the differential expression of a single gene is shown in Fig. 7. Here, the separation of 6m2 cells grown at two different temperatures and differentially labeled with tracking dyes is illustrated. 6m2 is a rat kidney cell line transformed by the temperature sensitive gene *gag-mos*. When the cells are grown at 33 °C, the P85gag-mos gene product transforms the cells. However, when the cells are grown at 39 °C, this protein is not produced and the cells express a normal phenotype. Fig. 7 shows that DEP–FFF is able to discriminate and fractionate 6m2 cells grown under these two conditions [81]. Thus, the effect of the differential expression of a single gene in genetically identical cells could be detected and the cells fractionated accordingly by DEP–FFF.

2) Dielectrophoretic–Magnetophoretic–FFF (MAP–DEP–FFF)—Immunomagnetic cell sorting (e.g., Dynal *IMS* or Miltenyi *MACS*) is a well-accepted approach to trapping cells with magnetically labeled surface markers in a high gradient magnetic field device while unmarked cells flow through uninhibited. Captured cells are subsequently released by physically removing the magnet. This method is useful for trapping cells having surface markers but it cannot discriminate between cells having varying densities of surface markers. To confer marker density discrimination, continuous magnetophoretic (MAP) sorting of

immunomagnetically labeled cells in a laminar flow profile has been demonstrated [82], [83]. In this scheme, cells are deflected by a quadrapole magnetic field in proportion to the degree of labeling and emerge from the sorting chamber along a trajectory that allows their differential recovery. While improved, that method uses unbalanced magnetic forces and is, therefore, highly flow-rate dependent and prone to trapping heavily labeled cells inadvertently. An alternative approach that is independent of flow-rate and more suitable for integrated microfluidic applications is DEP–MAP–FFF (see Fig. 8), a method [84] in which a balance of positive magnetophoretic and negative DEP forces is used to separate mixtures of differentially immunomagnetically labeled cells.

The magnetic force acting on a cell can be assumed to result from the combined effect of n identical immunomagnetic labels bound to it and can be written as

$$\overline{F}_{\mathrm{MAP}} = n\varphi \overline{G}_{\mathrm{MAP}} B_0^2 \tag{8}$$

where φ is a constant for a given magnetic label and the magnetic field gradient has been written as a geometry term G_{MAP} times the magnetic flux density B_0. Note that when flux density is sufficiently large, the magnetization of immunomagnetic beads saturates, and

$$\overline{F}_{\mathrm{MAP}} = n\,\Psi\,\overline{G}_{\mathrm{MAP}} B_0 \tag{9}$$

where Ψ reflects the saturated magnetic polarization of each bead. In this case, the magnetic force depends only on the magnetic field gradient. While (8) and (9) apply to the magnetic capture of cells by immunomagnetic cell selection [85], the goal in DEP–MAP–FFF is *not to trap the cells*. In this method, a DEP–FFF separation chamber sits on a periodically varying magnetically polarizable layer that itself overlays a flat magnet (Fig. 8). This construction gives rise to a magnetic field having well-defined spatial inhomogeneity which leads to a MAP force that falls with height above the chamber floor but is on average constant throughout the separation chamber at any given height. The MAP force pulls immunomagnetically labeled cells toward the electrode plane until the sum of the downward MAP and sedimentation forces are balanced by the levitating DEP force provided by electrical excitation of the electrode array. The balance of forces that determines the particle equilibrium height is

$$\overline{F}_{\mathrm{MAP}} + \overline{F}_{\mathrm{gravity}} + \overline{F}_{\mathrm{DEP}} = 0 \tag{10}$$

which, using the same notation as before, can be expressed as

$$\begin{aligned} n\,\Psi\,\overline{G}_{\mathrm{MAP}} B_0 e^{-h/h_{\mathrm{MAG}}} + [\,\upsilon(\rho_p - \rho_s) + \mathrm{nm}_{\mathrm{label}}\,]g \\ + 2\pi\varepsilon_m r^3 \mathrm{Re}(f_{\mathrm{CM}}) \mathrm{ApE}_{\mathrm{RMS}}^2 e^{-2\pi h/d} = 0 \end{aligned} \tag{11}$$

where m_{label} is the mass of each immunomagnetic label. If the magnetic labeling is zero ($n \rightarrow 0$), this equation reduces to the plain DEP–FFF equation. Therefore, not only do unlabeled cells behave in a well-defined manner but also a DEP–MAP–FFF separator chamber may be used for ordinary DEP trapping and DEP–FFF separations, providing versatility in functionality. If the cells are heavily immunomagnetically labeled and the MAP force dominates the downward force in (11), the resulting decrease in levitation height h is approximately proportional to the logarithm of the number n of magnetic labels attached to the cells. This allows for the discrimination of a wide range of immunomagnetic labeling concentrations for a given setting of the device.

The applied electric field E_{RMS} and frequency can be adjusted to control the DEP force opposing the MAP force, eliminating the need to alter the magnetic field and rendering the discriminating power of the method electrically programmable in analogy with the DEP–FFF case. Finally, much smaller magnetic forces are needed in DEP–MAP–FFF than in immunomagnetic cell selection, allowing lighter and less expensive magnets to be used. All of these factors are advantageous for use in GSAP devices.

C. Other Variants of DEP Trapping and DEP–FFF

An apparatus and method in which particles are directed, in accordance with their dielectric crossover frequencies, into multiple testing bays positioned alongside a flow channel, has been described by Pethig *et al.* [86]. This approach utilizes multiple sets of electrodes disposed along the length of a channel that are used to temporarily withhold different particle types from a flowing mixture and subsequently allows them to be moved over into the test bays by crosswise fluid flow after the DEP field has been removed. Particles entering the channel initially experience negative DEP and flow along the channel over electrode sets energized by different frequencies until they encounter a set that provides a sufficiently positive DEP force to withhold them from the flow stream. As we described earlier, cells typically exhibit negative DEP at low frequencies and positive DEP above a characteristic crossover frequency. Therefore, different cell types will tend to be withheld at different locations in the channel if subsequent electrode segments are excited by progressively higher frequencies.

A variant of DEP–FFF, which has been under development and testing at M.D. Anderson Cancer Center, Houston, TX, for several years and dubbed the *electrosmear*, uses a microscope slide coated with a strong cell-binding agent and patterned with either a continuous or segmented interdigitated electrode array. A flow channel is configured along the length of the slide. A cell mixture entering the flow channel from one end is initially subjected to hyperlayer–DEP–FFF induced by a negative DEP force from the electrodes. In a continuous electrode configuration, the applied frequency is increased with time as the sample experiences DEP–FFF separation along the slide. When the frequency approaches the crossover frequency for each different cell type, and the sedimentation force acting on that cell type exceeds the DEP levitation force from the electrodes below, the cells touch down on the slide surface and are irreversibly captured by the binding agent. The positions at which different cell types are trapped depend on how the frequency is increased as the cells travel along the slide, and this can be programmed to vary with time to enhance the discrimination of selected cell types while deemphasizing others. In the case of multiple electrode segments, different frequencies may be applied and programmed for the different segments providing even more flexibility. Cells bound to the slides in either fashion are subjected to conventional staining by dyes or histochemical methods and to conventional examination by a pathologist or by a laser scanning cytometer. Different cell types are easily found because they are trapped in characteristic bands along the slide. The banding behavior for a number of normal and cancerous cell types is shown in Fig. 9 (C. Das, J. Noshari, and C. Joyce, unpublished data) together with a photograph showing a stained band of breast tumor cells separated from a blood sample by this method. Although these electrosmear methods may not appear to be very advanced compared with more sophisticated lab-on-a-chip designs, and are not applicable to GSAPs, they are valuable tools for interfacing with the existing diagnostic infrastructure and for demonstrating the effectiveness of dielectric sorting directly in “gold standard” diagnostic methods. Thus, they provide access for pathologists to dielectric methods in a familiar context and give a permanent record of the relationships between familiar cellular properties and cell dielectric phenotypes. Thus, we have found that the electrosmear breaks the language barrier between the physician and the lab-on-a-chip designer who is attempting to develop chip-scale separations of complex cell mixtures. A very similar approach to the multiple segment method for trapping cells on a

slide, evidently developed entirely independently from our effort, was recently reported by Holmes and Morgan [87].

While DEP–FFF exploits a balance between opposing sedimentation and DEP forces, these forces may also be usefully exploited when applied orthogonally. Thus, Becker *et al.* [88] and Holmes and Morgan [87] have demonstrated fractionation by exploiting the sedimentation properties of cells whose horizontal positions within hydrodynamic flow profiles are maintained by DEP forces. These methods are readily applicable to GSAP devices.

IV. DEP–MEDIATED CELL FOCUSING

A. DEP Deflection

As we have seen, negative DEP forces can be used to position particles within flow streams. This effect can be usefully employed where particles need to be focused at predetermined locations to allow measurements. For example, multiple electrodes have been used to apply sequential or opposing DEP forces to deflect particles within diffuse flows into well-ordered streams for subsequent trapping [89], [90] prior to impedance sensing [46], and for optical analysis. Unbalanced DEP forces may also be used to deflect, rather than focus, the trajectories of particles in a flow stream in accordance with particle dielectric properties in order to separate the different types. However such schemes are highly flow-rate dependent and critically dependent on the initial positions of particles upstream of the DEP deflection elements and controlling these factors adequately may impose unrealistic constraints for microfluidic systems.

Finally, in a deflection-based variant of the hyperlayer DEP–FFF method, traveling wave DEP has been combined with DEP levitation to allow lateral displacement of particles based on the imaginary part of their dielectric permittivity [91].

B. Multipole Traps

Negative DEP forces can be used to spatially confine particles in traps. An inhomogeneous electric field distribution generated by four or more electrodes creates a potential energy minimum in which particles are focused and retained. Such traps have been examined in detail by Fuhr and colleagues for both cells and bacteria [90], [92], [93] and by Hughes and Morgan for viruses [94], [95]. Recent derivatives of this confinement method that use multiple DEP traps include an array cytometer by Voldman *et al.* [96]. Using this method, a single cell may be trapped in each of many traps and the differential responses of the cells upon exposure to different drug or toxicant challenges can be studied simultaneously via optical methods.

Such multipole traps are useful for capturing and holding cells under electronic control, perhaps for biosensor applications. However, the requirement for the potential well to be sufficiently deep to constrain the particles against fluid flow means that such devices must operate under DEP conditions far from particle crossover frequencies, and this largely precludes their application for sorting or discrimination unless particle types are dramatically different.

C. Spiral Electrodes

A spiral electrode configuration (see Fig. 10) can be used to exploit DEP attraction and repulsion in conjunction with traveling wave DEP to concentrate cells [50], [97], [98]. A typical spiral array consists of four parallel electrode elements that are energized by signals of the same frequency but phases of 0°, 90°, 180°, and 270° to create a concentric traveling field that sweeps toward the center of the spiral. Excitation by phases 0°, 270°, 180°, and 90° results in a field that sweeps outward toward the periphery of the spiral. Signals of 0°, 180°, 0°, and 180° phases produce a stationary field pattern that can be used for DEP trapping, levitation, or, at

higher applied fields, cell bursting. In collaboration with Chulabhorn Research Institute, Bangkok, Thailand, we have demonstrated differential cell trapping and focusing (see Fig. 11). Human erythrocytes infected by the malarial agent *Plasmodium falciparum* were discriminated from uninfected cells and focused from a scattered state to the center of a spiral [50]. One advantage of this method is that it simultaneously exploits both the real and imaginary dielectric properties of the cells. Generally, the traveling wave DEP velocity is a maximum when cells are close to their crossover frequency, in principle conferring much higher discrimination to this form of separation than if either parameter is used alone. Unfortunately, the forces derived from the traveling wave component tend to be very small and unable to resist hydrodynamic forces from fluids flowing at low rates. Therefore, focusing by spiral electrodes is best suited to static conditions, making target fraction removal difficult. Nevertheless, the high discrimination of the method makes it attractive where target particle analysis can be accomplished *in situ*.

V. AC IMPEDANCE DETECTION OF PARTICLES

Although this chapter focuses on sample manipulation by ac electrokinetic methods, it is useful to mention a detection method that depends on the same underlying particle dielectric properties as ac electrokinetic methods and that can be readily integrated into GSAP devices, namely, particle impedance sensing. The impedance of a small array of sensing electrodes filled with liquid suspension will change when a particle passes through it. The ac impedance spectrum of the particle can be determined if ac electrical signals at several different frequencies are applied to the electrodes and the resultant signal is deconvoluted to reveal its real and imaginary components at the different frequencies. The impedance spectrum indicates not only the particle size but also its dielectric properties in accordance with the earlier discussion of f_{CM} The method may be thought of as an extension of the ac Coulter technique for electronically counting particles.

Fig. 12 shows a scheme that we have applied to this type of analysis [44], [45], [99]. The desired frequencies are downloaded as a Fourier sum waveform to an arbitrary waveform generator. An analog–digital converter (ADC) acquires the sensor response and this is decimated by a field-programmable gate array (FPGA) derive in phase and out-of-phase frequency components. These allow particles to be sensed and counted and for their frequency response spectra to be deduced.

We have developed a sensing system that utilizes electrodes that are excited by up to eight simultaneous frequencies [45]. A similar scheme has been demonstrated independently by Gawad [46], who also exploited DEP particle focusing in his microsensors. This method has also been extended to the measurement of biomolecules by Sohn *et al.* [100].

While the simpler Coulter method is a *de facto* standard for benchtop particle analysis, that method only reveals particle size information, which is often insufficient for accurate particle differentiation. The multi frequency approach, on the other hand, can be used to elucidate information such as cell volume, cytoplasmic conductivity, membrane capacitance, cell viability and all the other factors that influence f_{CM}. With this discrimination, the method can distinguish between different cell types, as well as differentiate biological particles from contaminants. For these reasons, and because the impedance-sensing elements are necessarily microscale devices, multifrequency impedance sensing seems a worthy addition to the armament of dielectric methods applicable to GSAP devices. Finally, the method can be used to deduce particle concentrations without explicitly measuring fluid volumes, making it possible to accomplish particle counts without stringent fluid control or volume measurements.

VI. ELECTROMEDIATED LYSIS OF CELLS

Once a target cell subpopulation has been successfully isolated and, if desired, its surface markers have been characterized, subsequent molecular analyzes normally require that the cells be disrupted to release intracellular target analytes such as proteins, RNA, and DNA. Approaches to this include exposure to detergents or other lysing reagents or electrical lysis using large ac electric fields. DEP manipulations typically involve local electric fields less than 10^4 V/m and we have analyzed the conditions under which mammalian cells can sustain prolonged (40 min and longer) exposure to such fields without loss of viability or activity [66]. However, if it desired to electropermeabilize or disrupt cells, higher ac voltages may be applied. Depending on the cell type, at about 5×10^4 V/m, temporary membrane electropermeabilization occurs and this can be used to load reagents into cells. If the suspension conditions are gentle, the cells will reseal and maintain viability after such loading. However, above about 2×10^5 V/m, irreversible disruption of cell membranes occurs. We have shown that different cell types have characteristically different susceptibilities to destruction by ac electric fields. Fig. 13(a) shows the dependency of the disruption of human T-lymphocytes on field intensity and frequency of the applied electrical signal and Fig. 13(b) shows results for human MDA-MB-435 breast cancer cells (J. Schwartz, unpublished data). It is apparent that the cells burst in characteristic frequency and field ranges. This effect appears to arise because of breakdown of cell plasma membrane at field strengths of above ~4×10^9 V m^{-1}, corresponding to ~1.5 V across the 4-nm-thick lipid bilayer. Since the field that is imposed across the membrane by an applied ac electric field is frequency dependent (for the single shell dielectric model it is proportional to $Im(f_{CM})$), cells will exhibit electropermeabilization and electrobursting properties that reflect their ac electrokinetic fingerprints. Furthermore, in an inhomogeneous electric field, some cells will be excluded from the high field region. Clearly, a useful feature is the ability to select electrically whether to reversibly permeabilize or totally disrupt all, or select subpopulations, of cells. Electrobursting appears to be a good approach for releasing molecules from cells quickly and on demand from an electronic signal, and without the need to perfuse cells with lysis agents. Nevertheless, it is not clear that electrobursting can be applied effectively to disrupt all biological compartments of interest. Thus, nondielectric methods such as sonication may have to be used for spore disruption, for example.

VII. MOLECULAR MANIPULATIONS

A. Direct Molecular Trapping

The concentration of ions within the double layer surrounding a dissolved molecule falls exponentially with increasing distance from the surface with a characteristic Debye-Hückel [101] screening length, d, given by

$$d = \left(\frac{\varepsilon_m \mathrm{kT}}{8\pi n^0 z^2 e_0^2} \right)^{\frac{1}{2}} \tag{12}$$

where k is the Boltmann constant, T is the absolute temperature, n^0 is the bulk concentration of ions in the suspending medium, z is the (assumed balanced) valency of the suspending medium, and e_0 is the electronic charge. The ion concentration near the molecule will exceed the medium bulk concentration n^0, increasing the local electrical conductivity while the total charge in the double layer and, hence, the double layer capacitance, depends on the particle surface charge. A typical biomolecule has a minor axis dimension less than d and, consequently, the charge double layer occupies more volume than the molecule itself. Further, d increases with decreasing ionic concentration of the suspending medium but is independent of the

molecular size. Taken together, these factors assure that the DEP force on molecules in aqueous solution are always positive and that they are far more dependent on the solution conditions than on structural aspects of the biomolecules. Therefore, while direct DEP of molecular species in solution may usefully be employed for collecting molecules and, at a stretch, for discriminating between different classes of molecules, it does not offer the exquisite sequence- and structure-specific discrimation that is the basis for molecular diagnostics using DNA and proteins. Nevertheless, DEP collection and manipulation of DNA has been demonstrated some 15 years ago by Washizu [102]–[104] and more recently by Austin *et al.* [105] and, as with other ac electrokinetic techniques, the method has the advantage that it is electrically controllable.

B. DEP of Carrier Beads

It is at the molecular stage of sample preparation and analysis that the highest level of discrimination is needed in molecular diagnosis. Furthermore, as discussed earlier, once cells have been disrupted to release their molecular contents, agents are released that may directly interfere with assays, and proteases and nucleases may quickly begin to degrade the diagnostically important molecules. A useful approach that allows molecules to be collected and processed by DEP is based on the use of functionalized beads that trap molecules of interest. Then DEP can be used to manipulate the beads without the limitations inherent in direct DEP of molecules. Bead-based responses to molecules and to biofilms has been shown by Pethig *et al.* [106]

C. Dielectrically Engineered Carrier Beads

In many diagnostic applications, it is important to be able to identify more than one biomarker simultaneously. In order to accomplish this, some form of indexing system is required. In gene chips, each gene type is addressed via its coordinates on a spatial array. Such a system could also be employed in a GSAP; however, it would result in the need for a scanning optical system to measure the biomarkers and would impose difficult maintenance demands in cleaning or refreshing the array in a GSAP device made for reusable or continuous applications. Indexed beads carrying different probes or antibodies present one possible solution to these difficulties, since the beads could be measured by a chip-based cytometer stage. By disposing of the beads after each sample, running a blank between each sample, incorporating cleaning cycles, and using a new aliquot of sensitized beads for each and every assay, calibration issues can be addressed and the absence of carryover and cross-contamination can be verified. Placing the biologically active components on beads also means that a single, fluidic device can be applied to a wide range of sample preparation and molecular analysis problems by using different bead/probe combinations. Finally, because no biological components need to be attached to fixed surfaces within devices, those surfaces may be polytetrafluoroethylene (PTFE) coated, for example, to reduce biomolecular adhesion and carryover issues.

While fluorochromatic labeling is a possible solution to indexing the beads, it is possible that different classes of molecules might need to be processed by different techniques in the analysis stages of a GSAP. For example, RT–PCR, PCR, and ELISA methods might be needed for different molecular components. To enable this, the different bead types with their molecular targets should also have the capability of being independently manipulated and routed.

To make the efficient manipulation of beads electronically programmable, we have recently introduced molecular recognition and sensing elements that are attached to dielectrically indexed bead carriers that can be subjected to all forms of manipulation and discrimination discussed in earlier parts of this chapter. The ability to manipulate beads on a microscale also means that assays require minimal quantities of sample. For example, a bead of 5-μm diameter has the relatively large surface area of approximately 78 μm^2 yet occupies a volume of only

65 fL, about 1/15 that of a typical tumor cell. One hundred tumor cells and 250 beads composed of ten different bead types can be packed into a spherical region of 50 μm diameter using DEP-mediated focusing. This is the equivalent of almost 10^9 cells/ml held in contact with 2×10^9 beads/ml carrying molecular probes. After using the mixed beads in intimate contact with cells during the lysis step, they can be selectively manipulated according to each required processing procedure, including washing with protease and nuclease inhibitors and purging of potential assay inhibitors such as transition metals.

The structure of one type of dielectrically engineered microparticles developed by us as bead carriers for molecular sample preparation and analysis is shown in Fig. 14. The structure shown is biomimetic in the sense that the dielectric properties are qualitatively similar to those of mammalian cells. The microparticles comprise a very thin, dielectric surface layer covering a thin conductive shell of gold over a polystyrene core. The dielectric properties are defined by the size of the microparticles and the thickness and complex permittivity of the dielectric outer layer. We have utilized core particles ranging from 2.5 to 10 μm in diameter. The key to obtaining particles with well-defined dielectric properties lies in the fabrication of the surface dielectric layer, which must be of precisely defined thickness and uniformity. To obtain the structure shown, the gold conductive layer is first reacted with an alkanethiol to produce a covalently bound, self-assembled dielectric monolayer. The resulting hydrophobic particles are then exposed to vesicles of phospholipid to produce an additional, self-assembled layer on top of the alkanethiol layer. The resulting hybrid bilayer has hydrophilic phosphate head groups on the outside. We then take additional steps to make the bilayer resilient, to increase its surface charge, and to anchor molecular probes to its surface. The thickness of the bilayer can be precisely controlled simply by using alkanethiols and phospholipids having appropriate chain lengths. By varying the chain lengths, a library of different bead types can be made—each having different dielectric properties and each activated by attachment to different antibodies or probes. Fig. 15 shows the DEP crossover frequencies for four different microparticles fabricated by these methods. At sufficiently high frequencies, all bead types can be trapped by positive DEP to allow perfusion with reagent solutions or samples to be assayed. Unlike cells, the microparticles are not susceptible to osmotic damage and are less susceptible to electric field damage. This enables the electrodestruction of cells in the presence of probes and antibodies linked to bead carriers in order to trap one or more target molecules. After completion of molecular chemistries, differences in the dielectric properties of the beads can be used for multiplexed sorting and/or identification of molecular analytes. The design and characterization of dielectrically engineered beads has been reported in detail elsewhere [107].

VIII. DROPLET-BASED PROCESSORS

While the major focus of this chapter has been on sample preparation methods for fully programmable microTAS systems, it is also of interest to see what approaches are being developed to accomplish chemical and biomolecular analysis after the sample has been successfully prepared and its molecules have been released and cleaned. A conventional approach based on some of the concepts applied in clinical lab bench-scale fluidic machines is to use multiple fluid pathways through which sample and reagent streams are valved. Multiple pathways are easy to realize in fluidic systems, though valves represent a significant overhead in terms of complexity as well as issues such as dead space and sample carryover. Interesting variants in which multiple pathways are coupled with reagent and sample “accumulators” have also been successfully demonstrated. In our own studies, however, we were struck with the concept of digital processing of reagents in completely programmable ways. If reagents and samples can be “packaged” into minute droplets that are injected on demand from any one of a large array of reservoirs, and if these droplets can be moved about on demand on a two-dimensional (2-D) surface along arbitrarily chosen pathways where they

can be mixed, split, incubated, and measured, and if all of this can be accomplished under digital control from a programmable controller, then one has realized a programmable chemistry lab on a chip. Such a device would have almost unlimited potential for chemical synthesis and analysis.

The first practical suggestion for a device for moving small reagent droplets about on programmable paths by electrical means was made by Batchelder [108], [109], who conceived of a dielectrophoretic-based design. Unfortunately, this idea was ahead of its time in terms of manufacturing capabilities and appears never to have been realized. Subsequently Jones and Washizu [110] demonstrated a dielectric approach to moving droplets along fixed electrode tracks. This approach was extended to two dimensions by Kim *et al.* [111] and by Fair *et al.* [112], who have both demonstrated droplet processing concepts based on electrowetting. To accomplish fluid manipulation by electrowetting, fluid droplets are confined between a first (conducing) plate and second (dielectric) surface under which a set of electrodes is arrayed. By imposing a voltage between the plates, an electrically derived contact angle gradient is produced that drives fluid movement over the dielectric surface. The method depends on wetting the dielectric surface and direct electrical contact between the solution and one electrode.

Concerned with the need for conductive solutions and contamination issues for amphiphilic biomolecular species resulting from deliberately wetting a semihydrophobic surface, our laboratory has focused on using DEP for fluid handling in a somewhat more sophisticated manner [113] than proposed by Batchelder. The DEP force arises from the energy decrease that occurs when polarizable material moves into an electrical field. Therefore, contact with either an electrode or dielectric surface is not required and can, in principle, be eliminated. This allows droplets of any size to be manipulated, which offers special advantages in nano droplet injection, mixing, and titrations [114]. The sizes of droplets that have been programmably moved about on 2-D surfaces and mixed or split range from nano to microliter, and, using DEP injection, droplets as small as 10 pL have been titrated into larger droplets [114], [115]. Under DARPA sponsorship and in collaboration with Lawrence Livermore National Laboratory, the University of California, Davis, Coventor Inc., and Lynntech Inc., we have developed a completely integrated droplet processor that has a processing surface containing CMOS logic and switching for a 32 × 32 array of electrodes, providing for a scaleable solution to droplet processing. Our device contains maintenance ports to allow cleaning and recharging of the device as required.

Assays run on droplet processors are linear and the technology offers the possibility for parallel processing of samples as well as for intelligent processing whereby the results of one assay are used to intelligently trigger a tree of additional assays using choices of reagents from multiple injector reservoirs according to assay outcomes. In view of the flexibility of such devices, it seems highly likely that these will eventually insinuate themselves into many analysis and control systems in our daily lives as well as forming programmable analysis stages for GSAP devices as envisioned here.

IX. CONCLUSION

As stated at the outset, the goal of this work is to develop integrated fluidic devices able to sort, isolate, and burst target cells from clinically relevant samples and to execute molecular marker assays on them rapidly and automatically. This requires that sample preparation issues be addressed—we have, therefore, described several enabling technologies based on DEP that can accomplish key processing steps. These enabling technologies (see Fig. 16) can be combined in a sequential, flow-through fashion to create a complete system. The key feature of the approach is the ability to manipulate, discriminate, and isolate target particles and cells

within their suspending medium, to perfuse them as necessary with reagents for target marker enumeration, to liberate target molecules from within them, and to capture and clean these molecules, and to present the target molecular disease markers to a detection system on dielectrically indexed carrier beads for programmable analysis. Although the physics may appear knotty, the devices needed to accomplish DEP and MAP manipulations are straightforward, robust, and inexpensive, and DEP is electronically controlled and fully programmable. In addition to our efforts, several other groups are pursing DEP-based approaches to diagnostic problems. Pethig *et al.* [116] have been working a so-called "biofactory-on-a-chip," and recent books by Jones [117], Hughes [118], and Morgan and Green [119] describe DEP-based approaches to various sample handling and analysis problems. No doubt, other methods not relying on DEP will be developed for specific parts of the sample preparation and analysis sequence. Because of its flexibility and programmability, a successful design based on the principles of Fig. 16 will not be restricted in application to a single target disease but rather will be equally applicable to many diseases and many sample types. It appears, therefore, that for the first time in history a unified approach will become available for the detection and diagnosis of many diseases. If the manipulation and detection methods can be miniaturized as the prototype subunits suggest that they can be, then there appears to be no reason why molecular analysis for a multitude of diseases should not be made available at the point of care even in places lacking sophistication and infrastructure. This offers much promise not only for regions of our society having well-developed medical services but also for medically underserved communities even including the very poorest on the planet.

Acknowledgments

This work was supported in part by the Defense Advanced Research Projects Agency under Contract N66001-97-C-8608 and Grant DAAD19-00-1-0515 from the Army Research Office, in part by National Cancer Institute under Award 4R33 CA 88346-2, and in part by National Institute of Diabetes and Digestive and Kidney Diseases (NIDDK) under Award 5R01-DK56105-06.

REFERENCES

1. Wang XJ, Wang XB, Gascoyne PRC. General expressions for dielectrophoretic force and electrorotational torque derived using the Maxwell stress tensor method. J. Electrostatics 1997;vol. 39 (no 4):277–295.
2. Jones TB, Washizu M. Multipolar dielectrophoretic and electrorotation theory. J. Electrostatics 1996;vol. 37(no 1–2):121–134.
3. Clague DS, Wheeler EK. Dielectrophoretic manipulation of macromolecules: The electric field. Phys. Rev. E 2001;vol. 64(no 026605)
4. Pohl, HA. Dielectrophoresis: The Behavior of Neutral Matter in Nonuniform Electric Fields. Cambridge, U.K: Cambridge Univ. Press; 1978.
5. Gascoyne PR, Vykoukal J. Particle separation by dielectrophoresis. Electrophoresis 2002 July;vol. 23 (no 13):1973–1983. [PubMed: 12210248]
6. Ashkin A, Dziedzic JM. Optical trapping and manipulation of viruses and bacteria. Science 1987 Mar.;vol. 235(no 4795):1517–1520. [PubMed: 3547653]
7. Ashkin A, Dziedzic JM. Observation of radiation-pressure trapping of particles by alternating light beams. Phys. Rev. Lett 1985 Mar.;vol. 54(no 12):1245–1248. [PubMed: 10030975]
8. von Hippel, A. Dielectrics andWaves. Boston, MA: Artech House; 1995.
9. Freitag R, Schuegerl K, Arnold WM, Zimmermann U. The effect of osmotic and mechanical stresses and enzymic digestion on the electrorotation of insect cells (*Spodoptera frugiperda*). J. Biotechnol 1989;vol. 11(no 4):325–335.
10. Alder GM, Arnold WM, Bashford CL, Drake AF, Pasternak CA, Zimmermann U. Divalent cation-sensitive pores formed by natural and synthetic melittin and by Triton X-100. Biochim. Biophys. Acta 1991 Jan.;vol. 1061(no 1):111–120. [PubMed: 1899800]

11. Sukhorukov VL, Arnold WM, Zimmermann U. Hypotonically induced changes in the plasma membrane of cultured mammalian cells. J. Membrane Biol 1993;vol. 132(no 1):27–40. [PubMed: 8459447]
12. Wang XB, Huang Y, Gascoyne PR, Becker FF, Holzel R, Pethig R. Changes in Friend murine erythroleukaemia cell membranes during induced differentiation determined by electrorotation. Biochim. Biophys. Acta 1994 Aug.;vol. 1193(no 2):330–344. [PubMed: 8054355]
13. Huang Y, Wang XB, Becker FF, Gascoyne PR. Membrane changes associated with the temperature-sensitive P85gag-mos- dependent transformation of rat kidney cells as determined by dielectrophoresis and electrorotation. Biochim. Biophys. Acta 1996 June;vol. 1282(no 1):76–84. [PubMed: 8679663]
14. Gascoyne P, Pethig R, Satayavivad J, Becker FF, Ruchirawat M. Dielectrophoretic detection of changes in erythrocyte membranes following malarial infection. Biochim. Biophys. Acta—Biomembranes 1997;vol. 1323(no 2):240–252.
15. Huang Y, Wang XB, Holzel R, Becker FF, Gascoyne PR. Electrorotational studies of the cytoplasmic dielectric properties of friend murine erythroleukaemia cells. Phys. Med. Biol 1995;vol. 40(no 11): 1789–1806. [PubMed: 8587932]
16. Irimajiri A. A dielectric theory of “Multi-stratified shell” model with its application to a lymphoma cell. J. Theor. Biol 1979;vol. 78:251–269. [PubMed: 573830]
17. Chan KL, Gascoyne PR, Becker FF, Pethig R. Electrorotation of liposomes: Verification of dielectric multi-shell model for cells. Biochim. Biophys. Acta 1997 Nov.;vol. 1349(no 2):182–196. [PubMed: 9421190]
18. Gascoyne PRC, Becker FF, Wang XB. Numerical analysis of the influence of experimental conditions on the accuracy of dielectric parameters derived from electrorotation measurements. Bioelectrochem. Bioenerget 1995;vol. 36(no 2):115–125.
19. Grosse C, Schwan HP. Cellular membrane potentials induced by alternating fields. Biophys. J 1992;vol. 63(no 6):1632–1642. [PubMed: 19431866]
20. Arnold WM, Schwan HP, Zimmermann U. Surface conductance and other properties of latex particles measured by electrorotation. J. Phys. Chem 1987;vol. 91(no 19):5093–5098.
21. Green NG, Morgan H. Dielectrophoretic investigations of sub-micrometer latex spheres. J. Phys. D, Appl. Phys 1997;vol. 30(no 18):2626–2633.
22. Green NG, Morgan H. Dielectrophoretic separation of nano-particles. J. Phys. D, Appl. Phys 1997;vol. 30(no 11):L41–L44.
23. Markx GH, Huang Y, Zhou XF, Pethig R. Dielectrophoretic characterization and separation of microorganisms. Microbiology 1994;vol. 140:585–591.
24. Markx GH, Dyda PA, Pethig R. Dielectrophoretic separation of bacteria using a conductivity gradient. J. Biotechnol 1996;vol. 51(no 2):175–180. [PubMed: 8987883]
25. Fuhr G, Schnelle T, Hagedorn R, Shirley SG. Dielectrophoretic field cages: Technique for cell, virus and macromolecule handling. Cell. Eng 1995;vol. 1:47–57.
26. Hughes MP, Morgan H, Rixon FJ. Dielectrophoretic manipulation and characterization of herpes simplex virus-1 capsids. Eur. Biophys. J 2001 Aug.;vol. 30:268–272. [PubMed: 11548129]
27. Gascoyne PRC, Wang X-B, Huang Y, Becker FF. Dielectrophoretic separation of cancer cells from blood. IEEE Trans. Ind. Applicat 1997 May–June;vol. 33:670–678.
28. Archer S, Morgan H, Rixon FJ. Electrorotation studies of baby hamster kidney fibroblasts infected with herpes simplex virus type 1. Biophys. J 1999;vol. 76(no 5):2833–2842. [PubMed: 10233099]
29. Arnold, WM.; Jaeger, AH.; Zimmermann, U. The influence of yeast strain and of growth medium composition on the electrorotation of yeast cells and of isolated walls; Proc. DECHEMA Biotechnology Conf; 1989. p. 653-656.
30. Burt JPH, Chan KL, Dawson D, Parton A, Pethig R. Assays for microbial contamination and DNA analysis based on electrorotation. Annales de Biologie Clinique 1996;vol. 54(no 6):253–257. [PubMed: 8949422]
31. Egger M, Donath E, Ziemer S, Glaser R. Electrorotation—A new method for investigating membrane events during thrombocyte activation. Influence of drugs and osmotic pressure. Biochim. Biophys. Acta 1986 Sept.;vol. 861(no 1):122–130. [PubMed: 3092858]

32. Geier BM, Wendt B, Arnold WM, Zimmermann U. The effect of mercuric salts on the electro-rotation of yeast cells and comparison with a theoretical model. Biochim. Biophys. Acta 1987;vol. 900(no 1):45–55. [PubMed: 3297146]
33. Georgieva R, Neu B, Shilov VM, Knippel E, Budde A, Latza R, Donath E, Kiesewetter H, Baumler H. Low frequency electrorotation of fixed red blood cells. Biophys. J 1998;vol. 74(no 4):2114–2120. [PubMed: 9545070]
34. Gimsa J, Marszalek P, Loewe U, Tsong TY. Dielectrophoresis and electrorotation of neurospora slime and murine myeloma cells. Biophys. J 1991 Oct.;vol. 60(no 4):749–760. [PubMed: 1835890]
35. Griffith AW, Cooper JM. Single-cell measurements of human neutrophil activation using electrorotation. Anal. Chem 1998 July;vol. 70(no 13):2607–2612. [PubMed: 9666729]
36. Holzel R. Electrorotation of single yeast cells at frequencies between 100 Hz and 1.6 GHz. Biophys. J 1997;vol. 73(no 2):1103–1109. [PubMed: 9251826]
37. Huang Y, Holzel R, Pethig R, Wang XB. Differences in the AC electrodynamics of viable and nonviable yeast cells determined through combined dielectrophoresis and electrorotation studies. Phys. Med. Biol 1992 July;vol. 37(no 7):1499–1517. [PubMed: 1631195]
38. Kakutani T, Shibatani S, Senda M. Electrorotation of barley mesophyll protoplasts. Bioelectrochem. Bioenerget 1993;vol. 31(no 1):85–97.
39. Sukhorukov VL, Benkert R, Obermeyer G, Bentrup F-W, Zimmermann U. Electrorotation of isolated generative and vegetative cells, and of intact pollen grains of *Lilium longiflorum*. J. Membrane Biol 1998;vol. 161(no 1):21–32. [PubMed: 9430618]
40. Yang J, Huang Y, Wang X, Wang XB, Becker FF, Gascoyne PR. Dielectric properties of human leukocyte subpopulations determined by electrorotation as a cell separation criterion. Biophys. J 1999;vol. 76(no 6):3307–3314. [PubMed: 10354456]
41. Ziervogel H, Glaser R, Schadow D, Heymann S. Electrorotation of lymphocytes—The influence of membrane events and nucleus. Biosci. Rep 1986;vol. 6(no 11):973–982. [PubMed: 3580521]
42. Egger M, Donath E. Electrorotation measurements of diamide-induced platelet activation changes. Biophys. J 1995;vol. 68(no 1):364–372. [PubMed: 7711263]
43. Pethig R, Bressler V, Carswell-Crumpton C, Chen Y, Foster-Haje L, Garcia-Ojeda ME, Lee RS, Lock GM, Talary MS, Tate KM. Dielectrophoretic studies of the activation of human T lymphocytes using a newly developed cell profiling system. Electrophoresis 2002 July;vol. 23(no 13):2057–2063. [PubMed: 12210259]
44. Fuller, CK.; Hamilton, J.; Ackler, H.; Krulevitch, P.; Boser, B.; Eldredge, A.; Becker, F.; Yang, J.; Gascoyne, P. Microfabricated multi-frequency particle impedance characterization system. In: van den Berg, A.; Olthuis, W.; Bergveld, P., editors. Proc. Micro Total Analysis Systems. 2000. p. 265-267.
45. Yang J, Vykoukal J, Noshari J, Becker F, Gascoyne P. Dielectrophoresis-based microfluidic separation and detection systems. IJAMS 2000;vol. 3(no 2):1–12.
46. Gawad S, Schild L, Renaud Ph. Micromachined impedance spectroscopy flow cytometer for cell analysis and particle sizing. Lab. Chip 2001;vol. 1:76–82. [PubMed: 15100895]
47. Turcu I, Lucaciu CM. Dielectrophoresis—A spherical-shell model. J. Phys. A, Math. Gen 1989;vol. 22(no 8):985–993.
48. Kakutani T, Shibatani S, Sugai M. Electrorotation of nonspherical cells—Theory for ellipsoidal cells with an arbitrary number of shells. Bioelectrochem. Bioenerget 1993;vol. 31(no 2):131–145.
49. Wang X, Becker FF, Gascoyne PR. Membrane dielectric changes indicate induced apoptosis in HL-60 cells more sensitively than surface phosphatidylserine expression or DNA fragmentation. Biochim. Biophys. Acta 2002 Aug.;vol. 1564(no 2):412–420. [PubMed: 12175924]
50. Gascoyne P, Mahidol C, Ruchirawat M, Satayavivad J, Watcharasit P, Becker F. Microsample preparation by dielectrophoresis: Isolation of malaria. Lab. Chip 2003;vol. 2:70–75.
51. Pethig R, Kell DB. The passive electrical properties of biological systems: Their significance in physiology, biophysics and biotechnology. Phys. Med. Biol 1987 Aug.;vol. 32(no 8):933–970. [PubMed: 3306721]
52. Hu X, Arnold WM, Zimmermann U. Alterations in the electrical properties of T and B lymphocyte membranes induced by mitogenic stimulation. Activation monitored by electro-rotation of single cells. Biochim. Biophys. Acta 1990 Jan.;vol. 1021(no 2):191–200. [PubMed: 2302395]

53. Arnold WM, Geier BM, Wendt B, Zimmermann U. The change in the electrorotation of yeast-cells effected by silver ions. Biochim. Biophys. Acta 1986;vol. 889(no 1):35–48.
54. Ratanachoo K, Gascoyne PR, Ruchirawat M. Detection of cellular responses to toxicants by dielectrophoresis. Biochim. Biophys. Acta 2002 Aug.;vol. 1564(no 2):449–458. [PubMed: 12175928]
55. Pohl HA. Dielectrophoresis: Applications to the characterization and separation of cells. Methods Cell Separat 1977;vol. 1:67–169.
56. Mischel M, Rouge F, Lamprecht I, Aubert C, Prota G. Dielectrophoresis of malignant human melanocytes. Arch. Dermatolog. Res 1983;vol. 275(no 3):141–143.
57. Archer GP, Betts WB, Haigh T. Rapid differentiation of untreated, autoclaved and ozone-treated cryptosporidium parvum oocysts using dielectrophoresis. Microbios 1993;vol. 73(no 296):165–172. [PubMed: 8469175]
58. Fuhr G, Muller T, Baukloh V, Lucas K. High-frequency electric field trapping of individual human spermatozoa. Human Reproduct 1998;vol. 13(no 1):136–141.
59. Pimbley, DW.; Patel, PD.; Robertson, CJ. Environmental Monitoring of Bacteria. Dielectrophoresis. In: Edwards, C., editor. Methods in Biotechnology. Vol. vol. 12. Totowa, NJ: Humana; 1999. p. 35-53.
60. Heida T, Rutten WLC, Marani E. Dielectrophoretic trapping of dissociated fetal cortical rat neurons. IEEE Trans. Biomed. Eng 2001 Aug.;vol. 48:921–930. [PubMed: 11499529]
61. Lin IJ, Benguigui L. Dielectrophoretic filtration and separation: General outlook. Separat. Purificat. Methods 1981;vol. 10(no 1):53–72.
62. Lockhart NC. Dielectrophoresis in clay suspensions. Powder Technol 1983;vol. 35(no 1):17–22.
63. Wang XB, Huang Y, Burt JPH, Markx GH, Pethig R. Selective dielectrophoretic confinement of bioparticles in potential-energy wells. J. Phys. D, Appl. Phys 1993;vol. 26(no 8):1278–1285.
64. Markx GH, Talary MS, Pethig R. Separation of viable and nonviable yeast using dielectrophoresis. J. Biotechnol 1994;vol. 32(no 1):29–37. [PubMed: 7764449]
65. Becker FF, Wang XB, Huang Y, Pethig R, Vykoukal J, Gascoyne PR. Separation of human breast cancer cells from blood by differential dielectric affinity. Proc. Nat. Acad. Sci 1995;vol. 92(no 3): 860–864. [PubMed: 7846067]
66. Wang XJ, Yang J, Gascoyne PRC. Role of peroxide in AC electric field exposure effects on Friend murine erythroleukemia cells during dielectrophoretic manipulations. Biochim. Biophys. Acta, Gen. Subj 1999;vol. 1426(no 1):53–68.
67. Huang Y, Joo S, Duhon M, Heller M, Wallace B, Xu X. Dielectrophoretic cell separation and gene expression profiling on microelectronic chip arrays. Anal. Chem 2002 July;vol. 74(no 14):3362–3371. [PubMed: 12139041]
68. Milner KR, Brown AP, Betts WB, Goodall DM, Allsopp DW. Analysis of biological particles using dielectrophoresis and impedance measurement. Biomed. Sci. Instrum 1997;vol. 34:157–162. [PubMed: 9603031]
69. Brown AP, Betts WB, Harrison AB, O'Neill JG. Evaluation of a dielectrophoretic bacterial counting technique. Biosens. Bioelectron 1999 Mar.;vol. 14(no 3):341–351. [PubMed: 10230035]
70. Giddings JC. Field-flow fractionation: Analysis of macromolecular, colloidal, and particulate materials. Science 1993;vol. 260:1456–1465. [PubMed: 8502990]
71. Ratanathanawongs SK, Giddings JC. Dual-field and flow-progammed lift hyperlayer field-flow fractionation. Anal. Chem 1992;vol. 64:6–15. [PubMed: 1736679]
72. Cardot, PhJP.; Elgea, C.; Guernet, M.; Godet, D.; Andreux, JP. Size- and density-dependent elution of normal and pathological red blood cells by gravitational field-flow fractionation. J. Chromatog. B 1994;vol. 654:193–203.
73. Caldwell KD, Cheng Z-Q, Hradecky P, Giddings JC. Separation Of human and animal cells by steric field-flow fractionation. Cell Biophys 1984;vol. 6:233–251. [PubMed: 6085558]
74. Wang XB, Vykoukal J, Becker FF, Gascoyne PRC. Separation of polystyrene microbeads using dielectrophoretic/gravitational field-flow-fractionation. Biophys. J 1998;vol. 74(no 5):2689–2701. [PubMed: 9591693]

75. Huang Y, Wang XB, Becker FF, Gascoyne PRC. Introducing dielectrophoresis as a new force field for field-flow fractionation. Biophys. J 1997;vol. 73(no 2):1118–1129. [PubMed: 9251828]
76. Rousselet J, Markx GH, Pethig R. Separation of erythrocytes and latex beads by dielectrophoretic levitation and hyperlayer field-flow fractionation. Colloids Surf. A 1998;vol. 140(no 1–3):209–216.
77. Muller T, Schnelle T, Gradl G, Shirley SG, Fuhr G. Microdevice for cell and particle separation using dielectrophoretic field-flow fractionation. J. Liquid Chromatog. Relat. Technol 2000;vol. 23(no 1): 47–59.
78. Huang Y, Yang J, Wang XB, Becker FF, Gascoyne PRC. The removal of human breast cancer cells from hematopoietic CD34(+) stem cells by dielectrophoretic field-flow-fractionation. J. Hematother. Stem Cell Res 1999;vol. 8(no 5):481–490. [PubMed: 10791899]
79. Wang XB, Yang J, Huang Y, Vykoukal J, Becker FF, Gascoyne PRC. Cell separation by dielectrophoretic field-flow-fractionation. Anal. Chem 2000;vol. 72(no 4):832–839. [PubMed: 10701270]
80. Yang J, Huang Y, Wang XB, Becker FF, Gascoyne PRC. Differential analysis of human leukocytes by dielectrophoretic field-flow-fractionation. Biophys. J 2000;vol. 78(no 5):2680–2689. [PubMed: 10777764]
81. Vykoukal, J. Ph.D. dissertation, Grad. Sch. Biomed. Sci. Houston: Univ.Texas; 2001. Dielectrophoresis-based analyte separation and analysis.
82. Chalmers JJ, Haam S, Zhao Y, McCloskey K, Moore L, Zborowski M, Williams PS. Quantification of cellular properties from external fields and resulting induced velocity: Cellular hydrodynamic diameter. Biotechnol. Bioeng 1999 Sept.;vol. 64(no 5):509–518. [PubMed: 10404231]
83. Chalmers JJ, Haam S, Zhao Y, McCloskey K, Moore L, Zborowski M, Williams PS. Quantification of cellular properties from external fields and resulting induced velocity: Magnetic susceptibility. Biotechnol. Bioeng 1999 Sept.;vol. 64(no 5):519–526. [PubMed: 10404232]
84. Gascoyne, P.; Vykoukal, J.; Weinstein, R.; Gandini, A.; Parks, D.; Sawh, R. Magnetophoretic-dielectrophoretic field-flow fractionation. In: Baba, Y.; Shoji, S.; van den Berg, A., editors. Proc. Micro Total Analysis Systems. 2002. p. 323-325.
85. Nakamura M, Decker K, Chosy J, Comella K, Melnik K, Moore L, Lasky LC, Zborowski M, Chalmers JJ. Separation of a breast cancer cell line from human blood using a quadrupole magnetic flow sorter. Biotechnol. Prog 2001;vol. 17(no 6):1145–1155. [PubMed: 11735453]
86. Pethig, R.; Markx, GH. Apparatus and method for testing using dielectrophoresis. U.S. Patent 6 264 815. 2001 Jul 24.
87. Holmes, D.; Morgan, H. Dielectrophoretic chromatography of cells. In: Baba, Y.; Shoji, S.; van den Berg, A., editors. Proc. Micro Total Analysis Systems. 2002. p. 829-831.
88. Becker, FF.; Gascoyne, PRC.; Huang, Y.; Wang, X-B. Method and apparatus for fractionation using conventional dielectrophoresis and field flow fractionation. U.S. Patent 5 993 630. 1999 Nov. 30.
89. Fiedler S, Shirley SG, Schnelle T, Fuhr G. Dielectrophoretic sorting of particles and cells in a microsystem. Anal. Chem 1998;vol. 70(no 9):1909–1915. [PubMed: 9599586]
90. Muller T, Gradl G, Howitz S, Shirley S, Schnelle T, Fuhr G. A 3-D microelectrode system for handling and caging single cells and particles. Biosens. Bioelectron 1999;vol. 14(no 3):247–256.
91. De Gasperis G, Yang J, Becker FF, Gascoyne PRC, Wang XB. Microfluidic cell separation by 2-dimensional dielectrophoresis. Biomed. Microdev 1999;vol. 2(no 1):41–49.
92. Schnelle T, Hagedorn R, Fuhr G, Fiedler S, Muller T. Three-dimensional electric field traps for manipulation of cells—Calculation and experimental verification. Biochim. Biophys. Acta 1993 June;vol. 1157(no 2):127–140. [PubMed: 8507649]
93. Fuhr G, Reichle C, Muller T, Kahlke K, Schutze K, Stuke M. Processing of micro-particles by UV laser irradiation in a field cage. Appl. Phys. A, Mater. Sci. Process 1999;vol. 69(no 6):611–616.
94. Hughes MP, Morgan H. Dielectrophoretic trapping of single sub-micrometer scale bioparticles. J. Phys. D, Appl. Phys 1998;vol. 31(no 17):2205–2210.
95. Morgan H, Hughes MP, Green NG. Separation of submicron bioparticles by dielectrophoresis. Biophys. J 1999;vol. 77(no 1):516–525. [PubMed: 10388776]
96. Voldman J, Gray ML, Toner M, Schmidt MA. A microfabrication-based dynamic array cytometer. Anal. Chem 2002 Aug.;vol. 74(no 16):3984–3990. [PubMed: 12199564]

97. Wang XB, Huang Y, Wang X, Becker FF, Gascoyne PR. Dielectrophoretic manipulation of cells with spiral electrodes. Biophys. J 1997;vol. 72(no 4):1887–1899. [PubMed: 9083692]
98. Goater AD, Burt JPH, Pethig R. A combined travelling wave dielectrophoresis and electrorotation device: Applied to the concentration and viability determination of cryptosporidium. J. Phys. D, Appl. Phys 1997;vol. 30(no 18):L65–L69.
99. Ackler H, Krulevitch P, Miles R, Benett W, Swierkowski S, Malba V, Gascoyne PRC, Wang X-B, DeGasperis G. Microfluidic systems for electrochemical and biological studies. Proc. Electrochem. Soc 1998;vol. 14:54–61.
100. Facer GR, Notterman DA, Sohn LL. Dielectric spectroscopy for bioanalysis: From 40 Hz to 26.5 GHz in a microfabricated wave guide. Appl. Phys. Lett 2001;vol. 78(no 7):996–998.
101. Bockris, JO.; Reddy, AKN. Modern Electrochemistry. New York: Plenum; 1970.
102. Washizu M, Kurosawa O. Electrostatic manipulation of DNA in microfabricated structures. IEEE Trans. Ind. Applicat 1990 Nov.–Dec.;vol. 26:1165–1172.
103. Washizu M, Kurosawa O, Suzuki S, Shimamoto N. Applications of electrostatic stretch-and-positioning of DNA. IEEE Trans. Ind. Applicat 1995 May–June;vol. 31:447–456.
104. Kabata H, Okada W, Washizu M. Single-molecule dynamics of the Eco RI enzyme using stretched DNA: Its application to in situ sliding assay and optical DNA mapping. Jpn. J. App. Phys. 1, Regul. Pap. Short Notes 2000;vol. 39(no 12B):7164–7171.
105. Chou CF, Tegenfeldt JO, Bakajin O, Chan SS, Cox EC, Darnton N, Duke T, Austin RH. Electrodeless dielectrophoresis of single- and double-stranded DNA. Biophys. J 2002 Oct.;vol. 83(no 4):2170–2179. [PubMed: 12324434]
106. Zhou XF, Markx GH, Pethig R, Eastwood IM. Differentiation of viable and nonviable bacterial biofilms using electrorotation. Biochim. Biophys. Acta 1995;vol. 1245(no 1):85–93. [PubMed: 7654770]
107. Vykoukal J, Vykoukal DM, Sharma S, Becker FF, Gascoyne PRC. Dielectrically addressable microspheres engineered using self-assembled monolayers. Langmuir 2003 Mar.;vol. 19:2425–2433.
108. Batchelder JS. Dielectrophoretic manipulator. Rev. Sci. Instrum 1983;vol. 54(no 3):300–302.
109. Batchelder, JS. Method and apparatus for dielectrophoretic manipulation of chemical species. U.S. Patent 4 390 403. 1983 Jun 28.
110. Jones TB, Gunji M, Washizu M, Feldman MJ. Dielectrophoretic liquid actuation and nanodroplet formation. J. Appl. Phys 2001;vol. 89(no 2):1441–1448.
111. Lee J, Moon H, Fowler J, Schoellhammer T, Kim C-J. Electrowetting and electrowetting-on-dielectric for microscale liquid handling. Sens. Actuators A, Phys 2002 Jan.;vol. 95:259–268.
112. Pollack MG, Shenderov AD, Fair RB. Electrowetting-based actuation of droplets for integrated microfluidics. Lab. Chip 2002;vol. 2:96–101. [PubMed: 15100841]
113. Becker, FF.; Gascoyne, P.; Wang, X.; Vykoukal, JV.; De Gasperis, G. Method and apparatus for programmable fluidic processing. U.S. Patent 6 294 063. 2001 Sept. 25.
114. Vykoukal, J.; Schwartz, JA.; Becker, FF.; Gascoyne, PRC. A programmable dielectrophoretic fluid processor for droplet-based chemistry. In: Ramsey, JM.; van den Berg, A., editors. Proc. Micro Total Analysis Systems. 2001. p. 72-74.
115. Gascoyne, P.; Vykoukal, JV.; Schwartz, J.; Becker, FF. Apparatus and method for fluid injection. U.S. Patent Applicat. 20 020 063 060. 2002 May 30.
116. Zhou XF, Burt JPH, Talary MS, Goater AD, Pethig R. Development of biofactory-on-a-chip technology. Proc. SPIE Micromachining and Microfabrication 2000;vol. 4177:S6.
117. Jones, TB. Electromechanics of Particles. Cambridge, U.K: Cambridge Univ. Press; 1995.
118. Hughes, MP. Nanoelectromechanics in Engineering and Biology. Boca Raton, FL: CRC; 2002.
119. Morgan, H.; Green, N. AC Electrokinetics—Colloids and Nanoparticles. Baldock, U.K: Research Studies Press; 2003.

Biographies

Peter R. C. Gascoyne (Member, IEEE) received the Ph.D. degree in electronic materials science from the University of Wales, Bangor, U.K., in 1979.

He is a Professor in the Department of Molecular Pathology at the University of Texas M.D. Anderson Cancer Center, Houston. He is the author of more than 80 publications and an inventor on more than 20 patents. His research interest is the application of dielectric methods to cell analysis and sample manipulations in microfluidic diagnostic systems.

He is a Member of the EMBS Society.

Jody V. Vykoukal received the Ph.D. degree in biophysics from the Graduate School of Biomedical Sciences, University of Texas, Houston, in 2001.

Since 1993 he has been at the University of Texas M.D. Anderson Cancer Center, Houston, where he is currently a Research Associate in the Department of Molecular Pathology. His research interests include the application of dielectrophoresis to the separation and analysis of biological and biochemical analytes, particularly in fluidic microsystems.

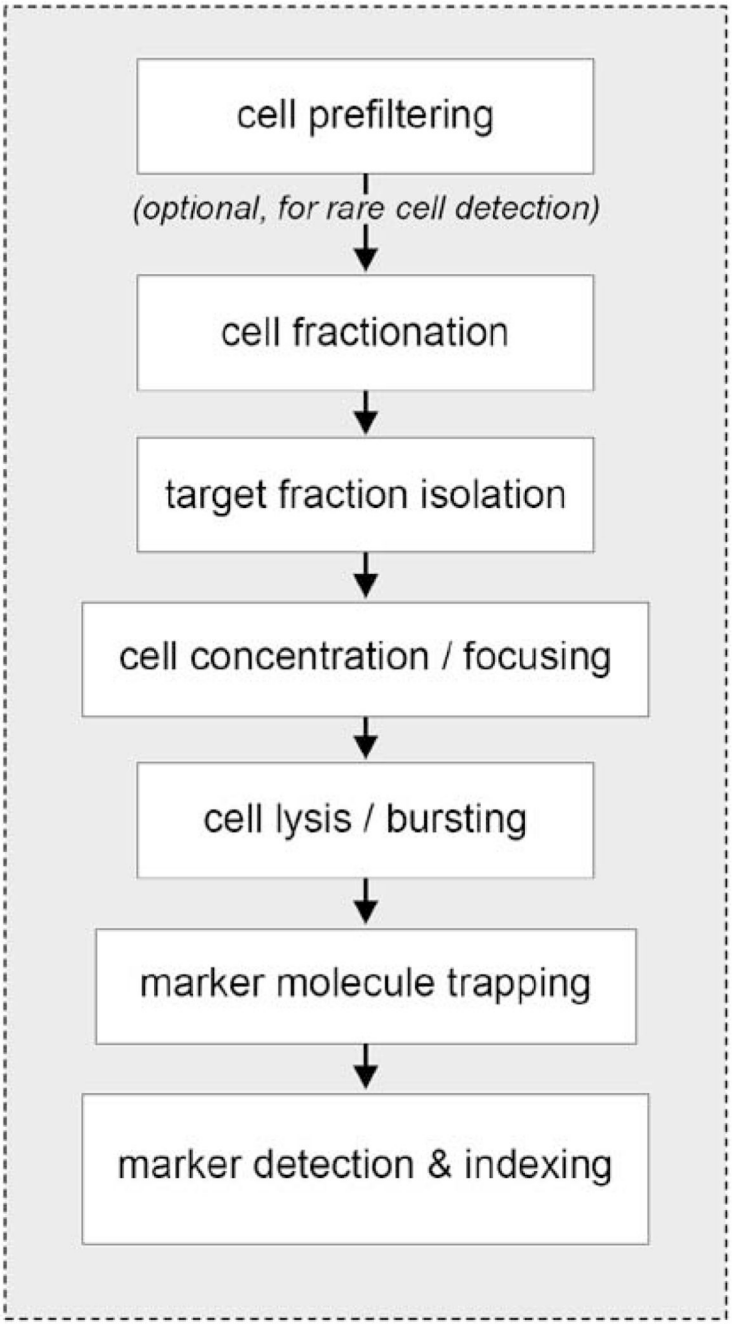

Fig. 1.
Steps necessary to perform molecular diagnostics on a raw sample.

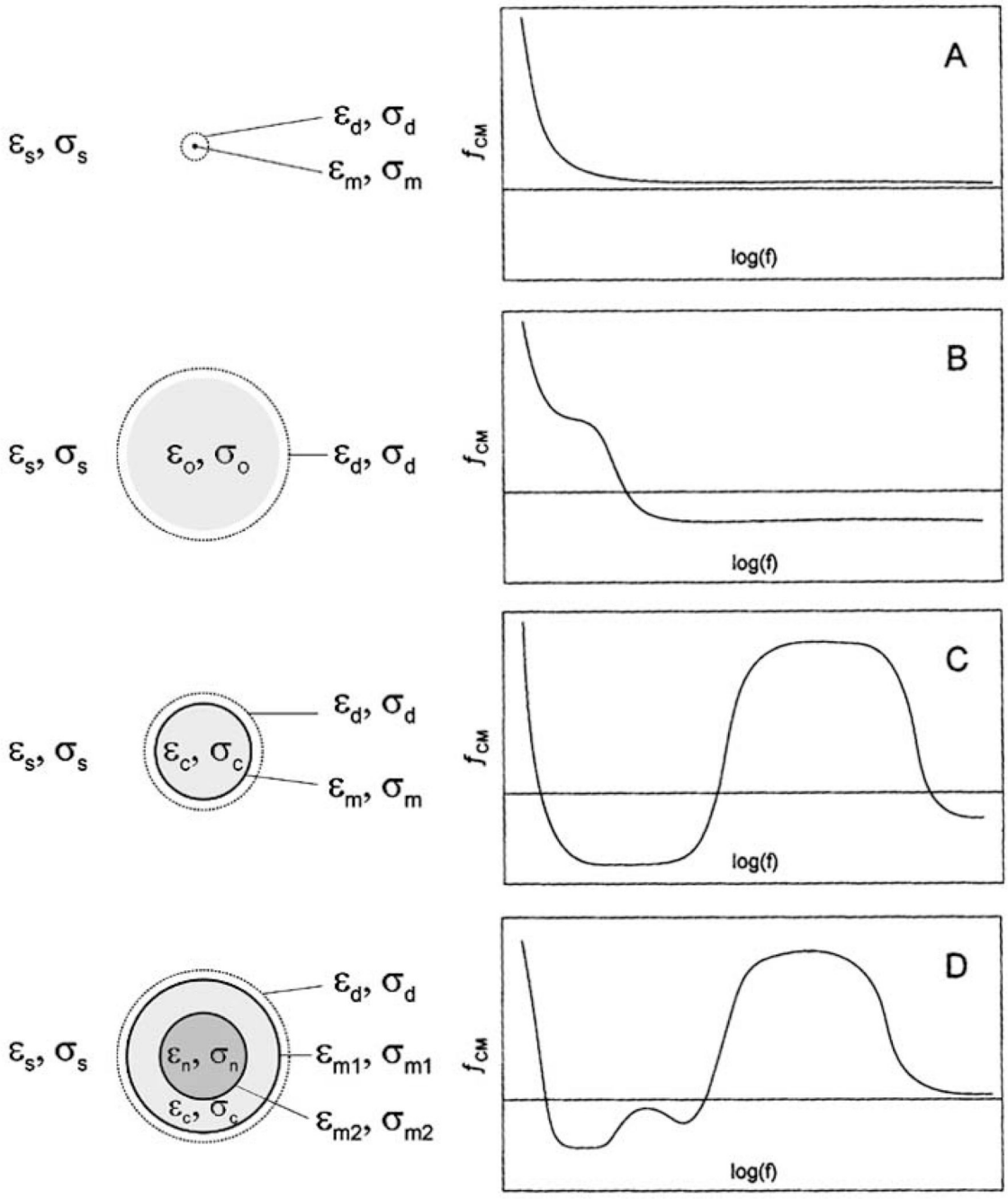

Fig. 2.
Simulated dielectrophoretic properties for: (a) point particles; (b) solid particles; (c) particles with a single compartment surrounded by a thin envelope; and (d) particles with two concentric compartments surrounded by thin envelopes.

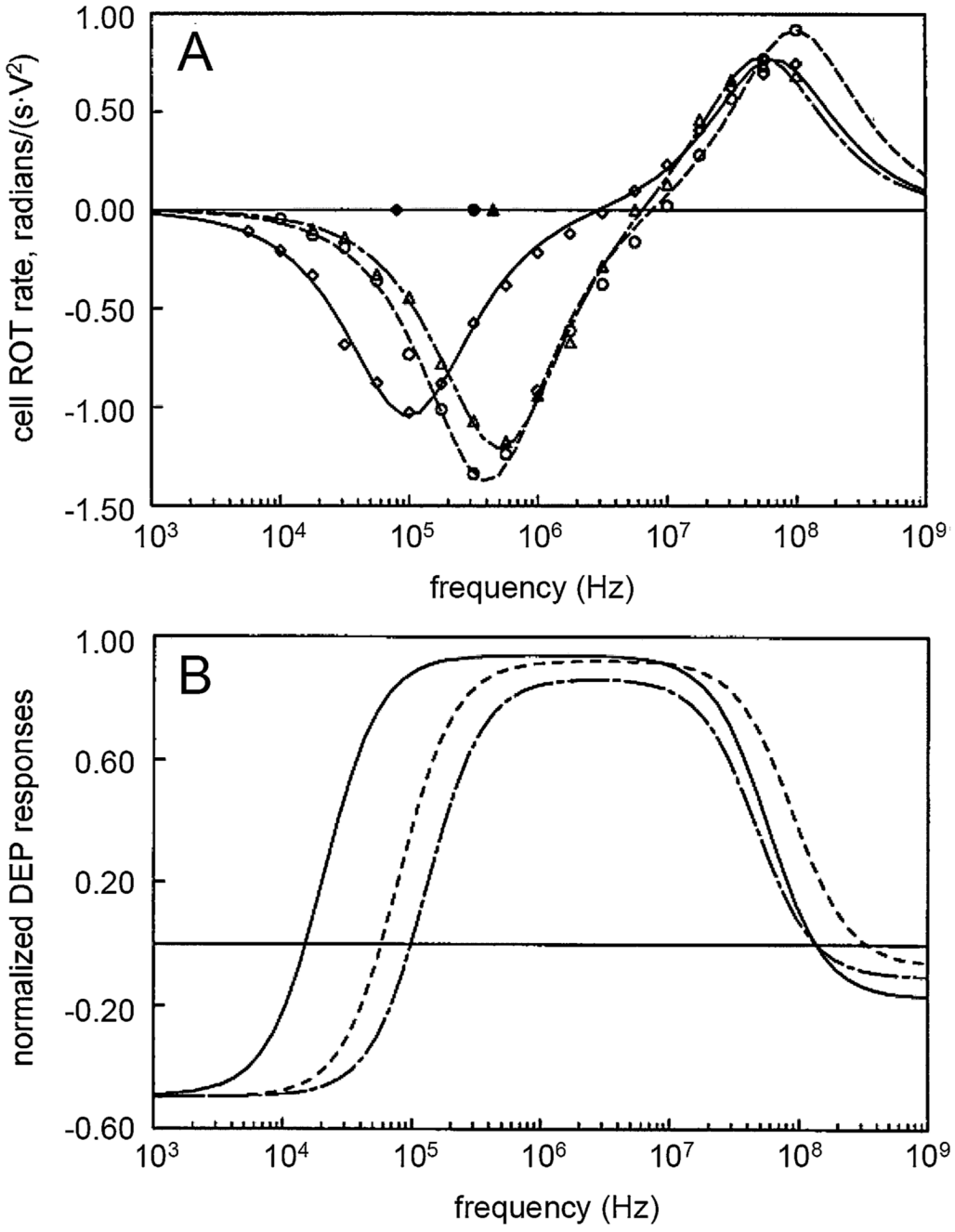

Fig. 3.

(a) Typical ROT spectra for human breast cancer cell line MDA231 (◊), T-lymphocytes (○), and erythrocytes (Δ) in isotonic sucrose of conductivity 56 mS/m. (b) DEP collection spectra for cell line MDA231 (—), T-lymphocytes (—), and erythrocytes (— -) in media of conductivity 10 mS/m calculated using the DEP parameters derived from the ROT measurements.

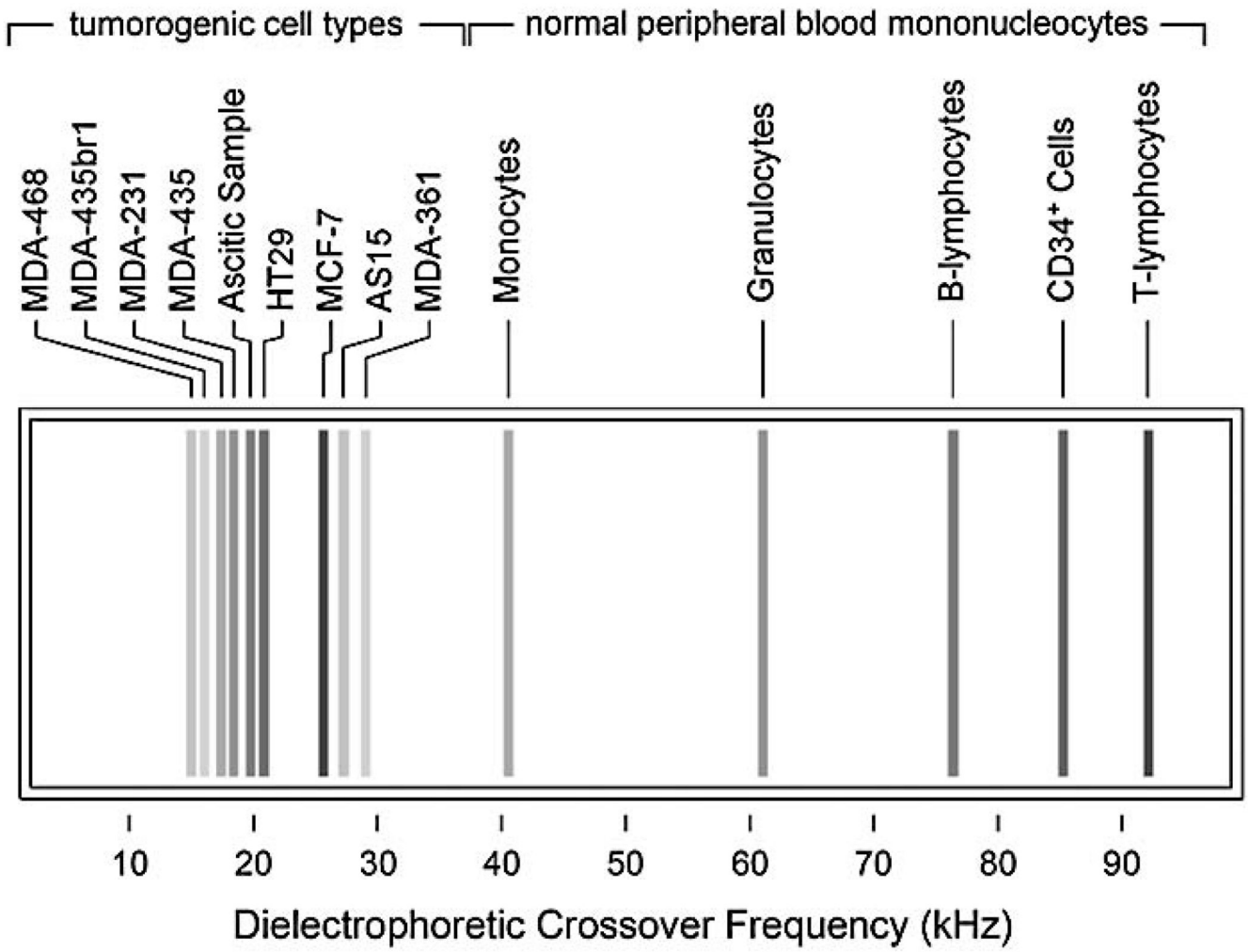

Fig. 4.
Comparison between DEP crossover data for nine human tumor cell types and normal peripheral blood mononuclear cells (medium conductivity 56 mS/m).

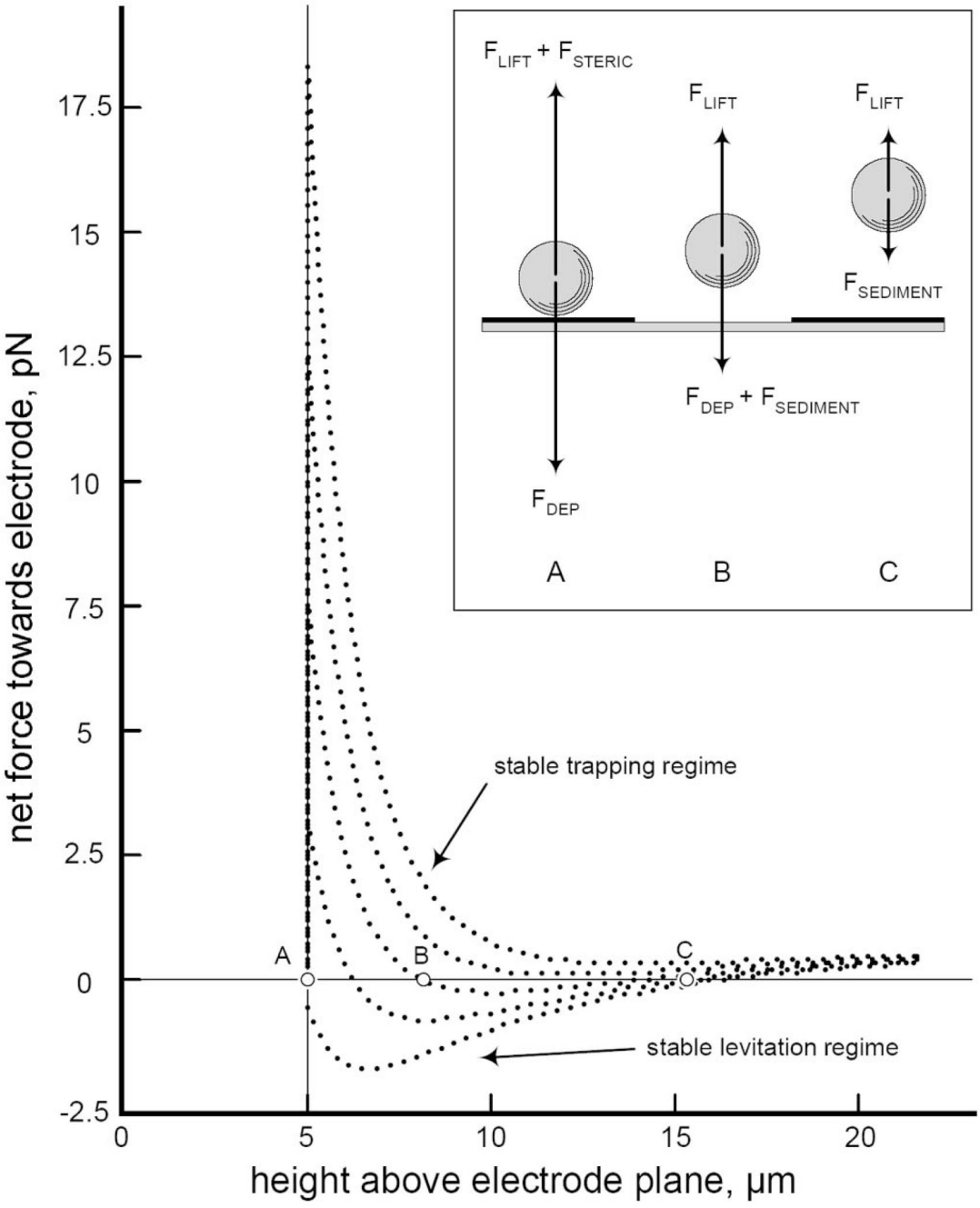

Fig. 5.

The sums of hydrodynamic lift, positive DEP, and sedimentation forces acting on a particle in a fluid flow stream are shown at five frequencies close to the crossover frequency. Between a stable trapping regime and a stable levitation regime, for which there are unique equilibrium positions, lies a regime characterized by multiple equilibrium positions. For example, the middle profile possesses the three equlibria that correspond to the balances of forces shown in the inset.

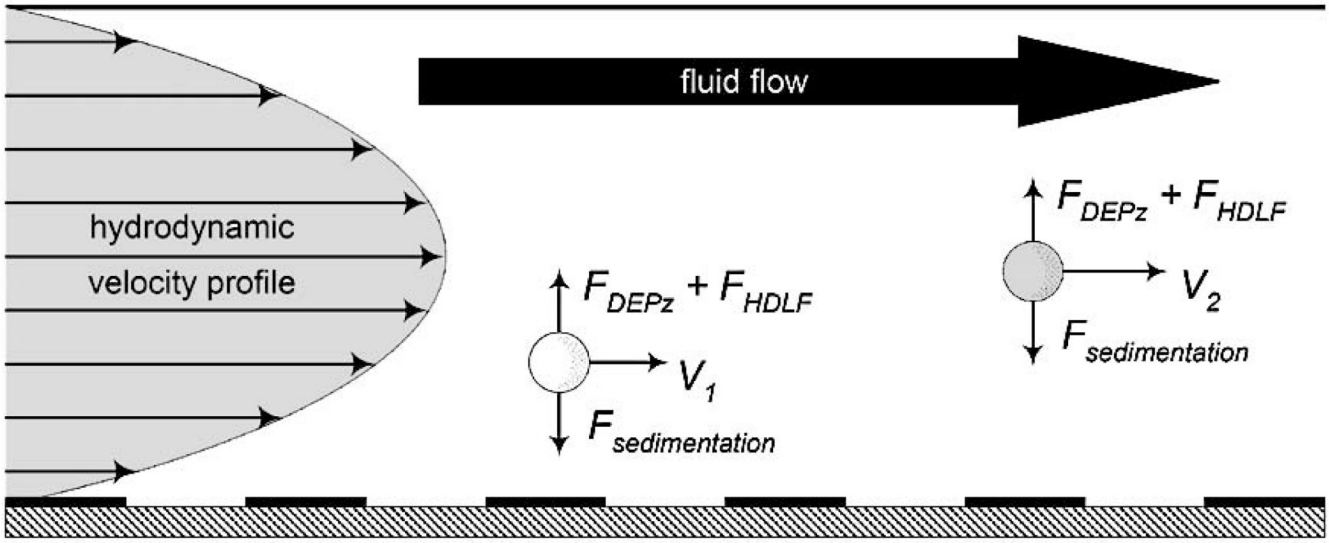

Fig. 6.
Principle of dielectrophoretic field-flow fractionation.

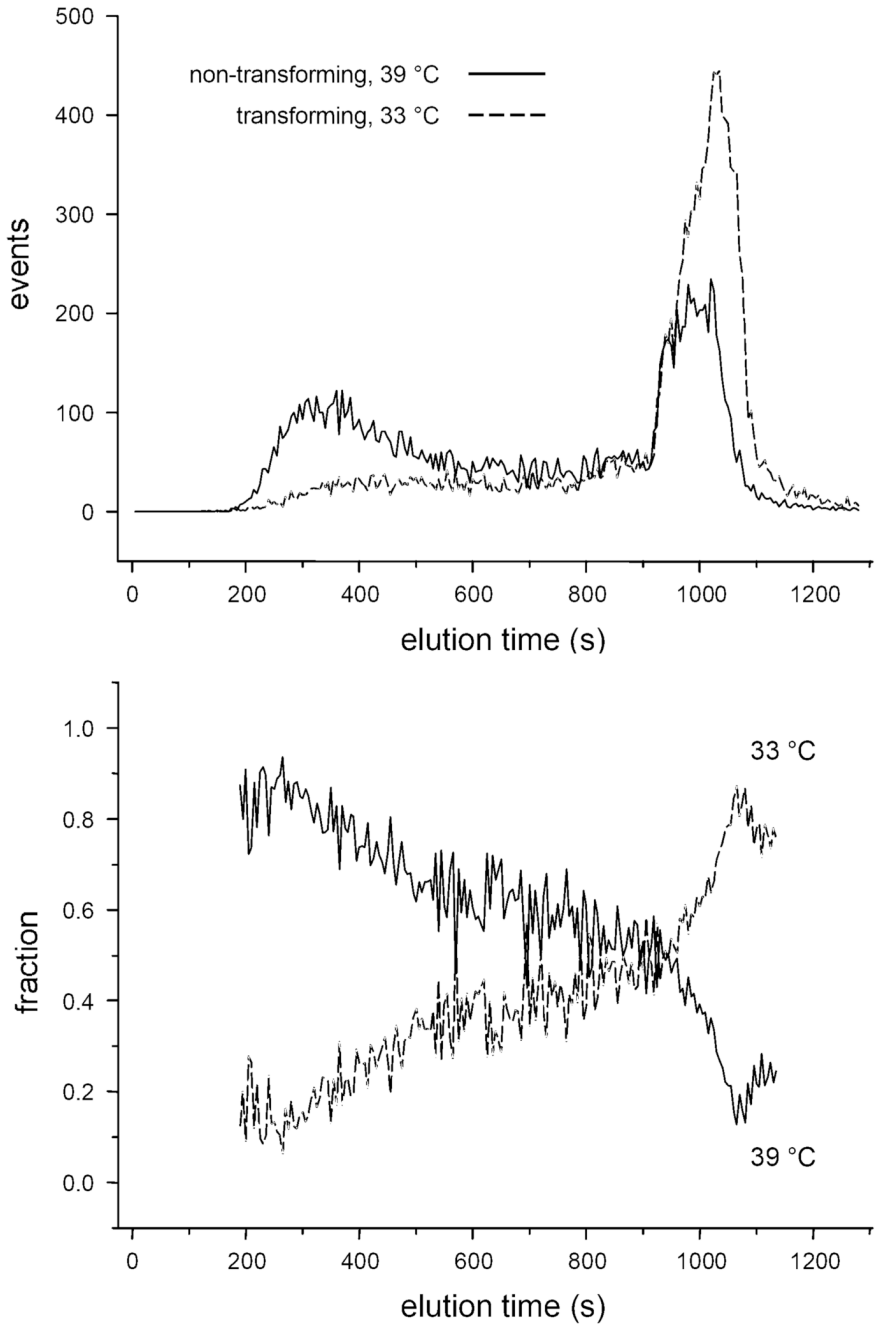

Fig. 7.

Separation of 6m2 cells using DEP–FFF. (a) Fractogram showing the separation of a mixed sample comprising 6m2 mutant rat kidney cells grown under transforming, 33 °C (- -) or nontransforming, 39 °C (—) culture conditions. (b) The dynamic purity of each separation was also evaluated by plotting, a function of time, the portion of cells in the eluate that were cultured under the different conditions as determined by fluorochrome prelabeling.

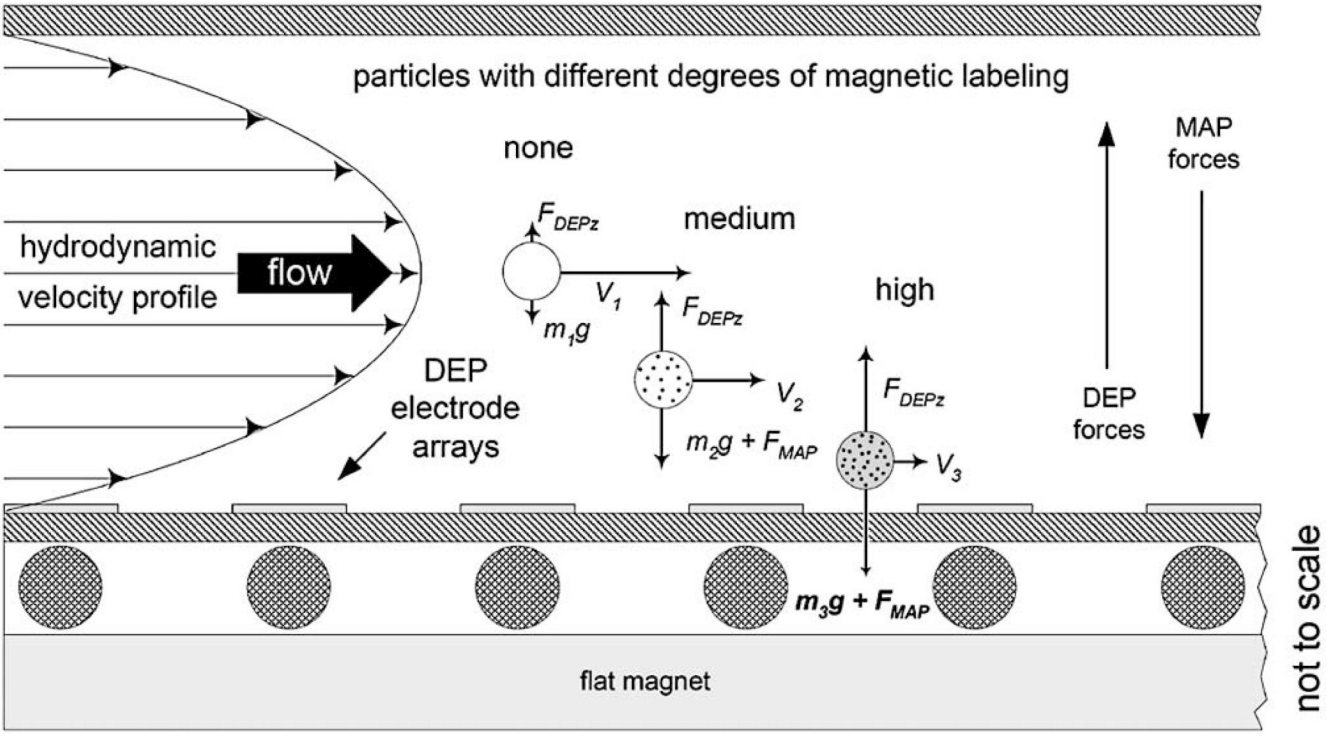

Fig. 8.
Principle of magnetaphoretic–dielectrophoretic field-flow fractionation.

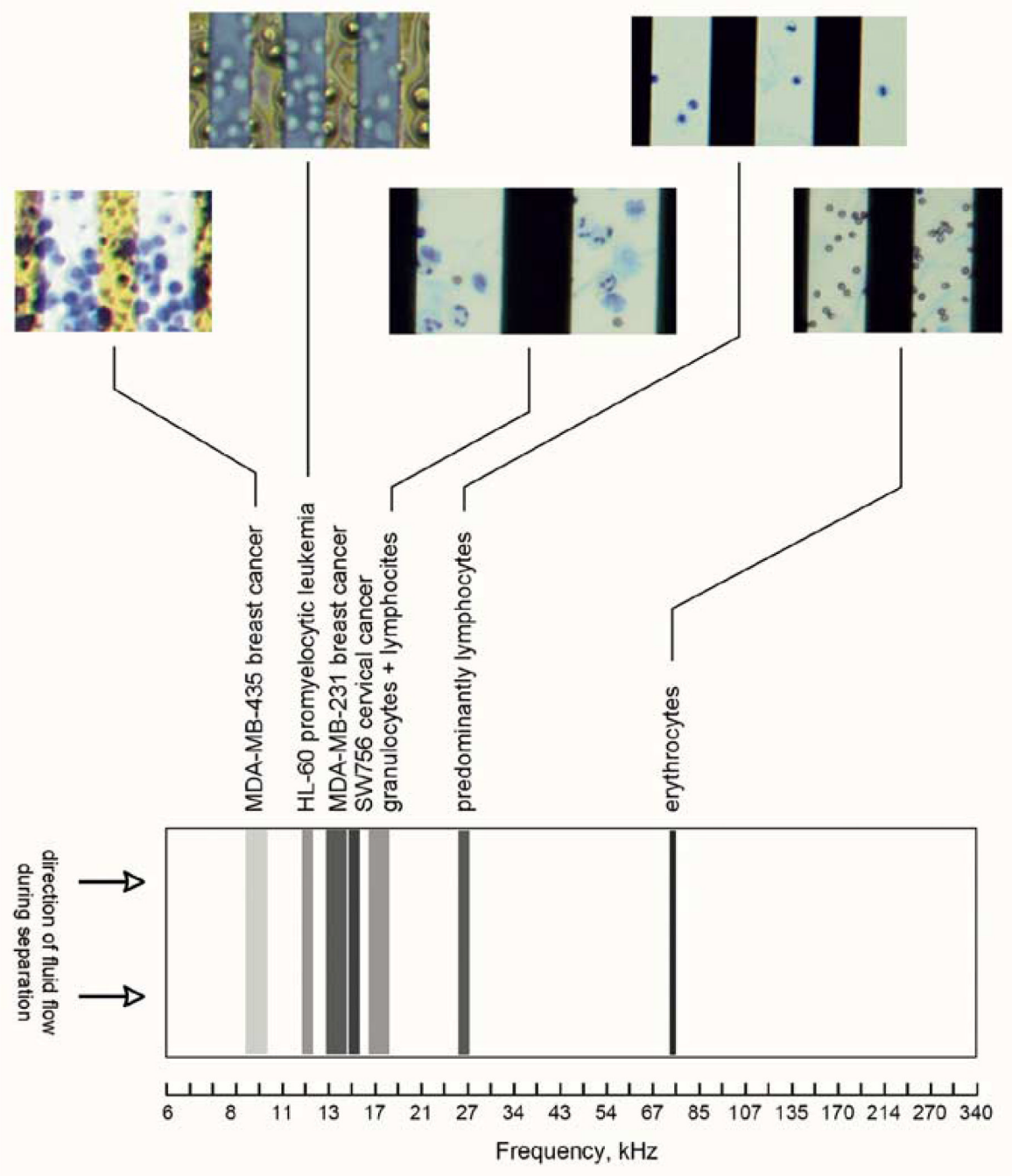

Fig. 9.
The electrosmear banding behavior for normal and cultured tumor cell types. The accompanying photographs show stained bands of cells from a mixed sample separation.

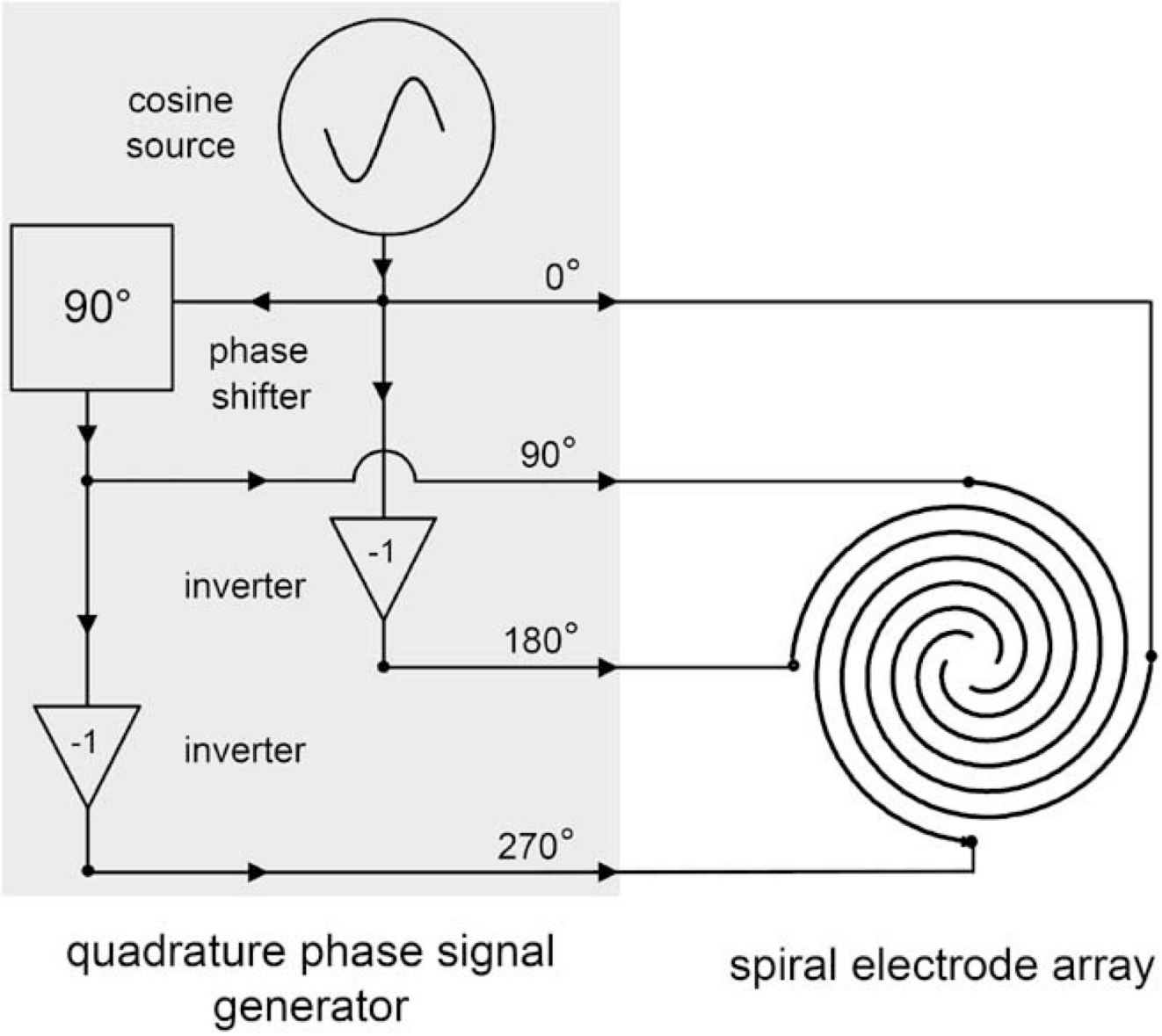

Fig. 10.
A spiral electrode array energized with a quadrature phase ac signal can be used to exploit DEP attraction and repulsion in conjunction with traveling wave DEP to concentrate cells.

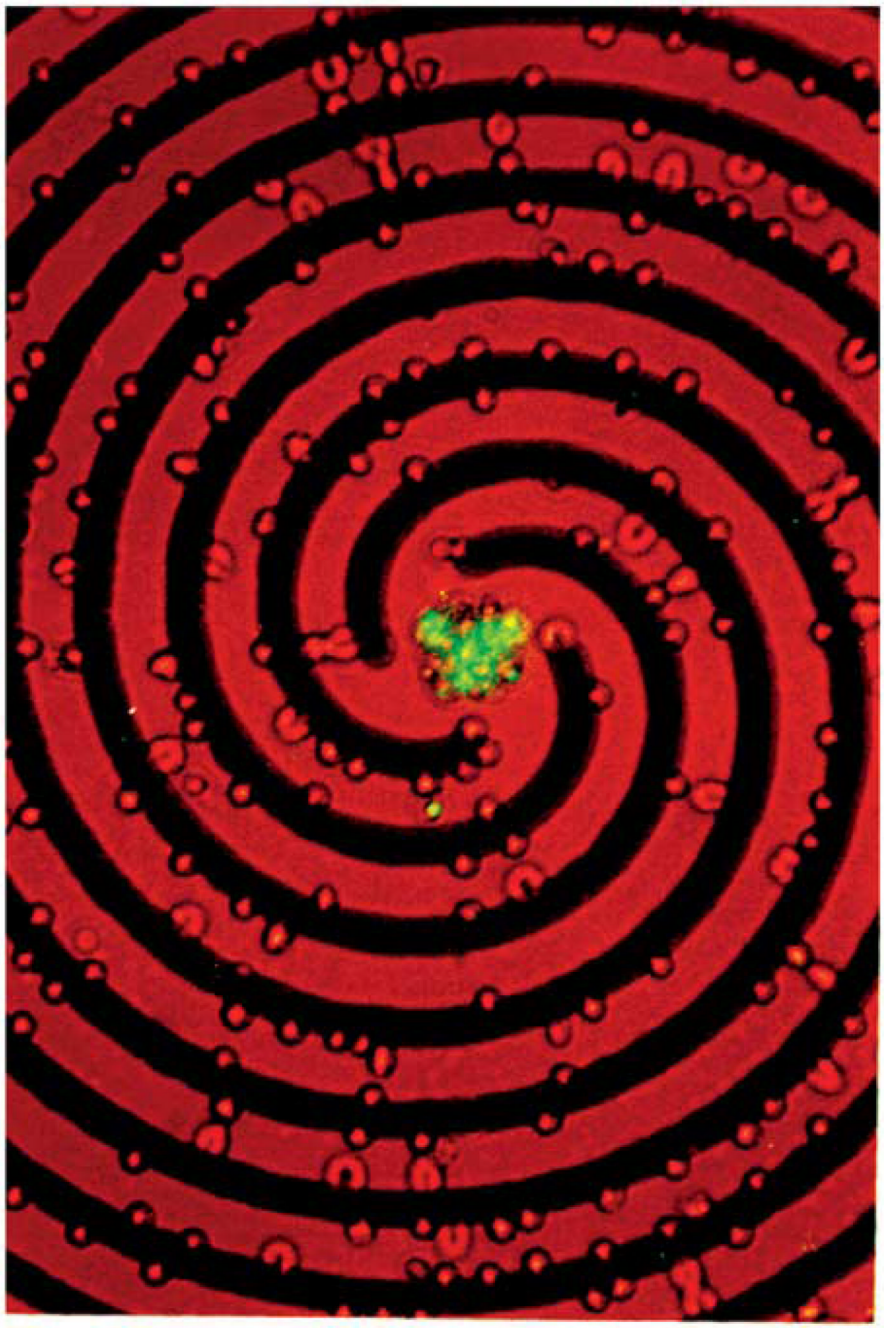

Fig. 11.
Cell trapping and focusing on a spiral traveling wave DEP electrode. Fluorescently labeled human erythrocytes infected by the malarial agent *Plasmodium falciparum* have been have been discriminated from uninfected cells and focused from a scattered state to the center of the spiral electrode.

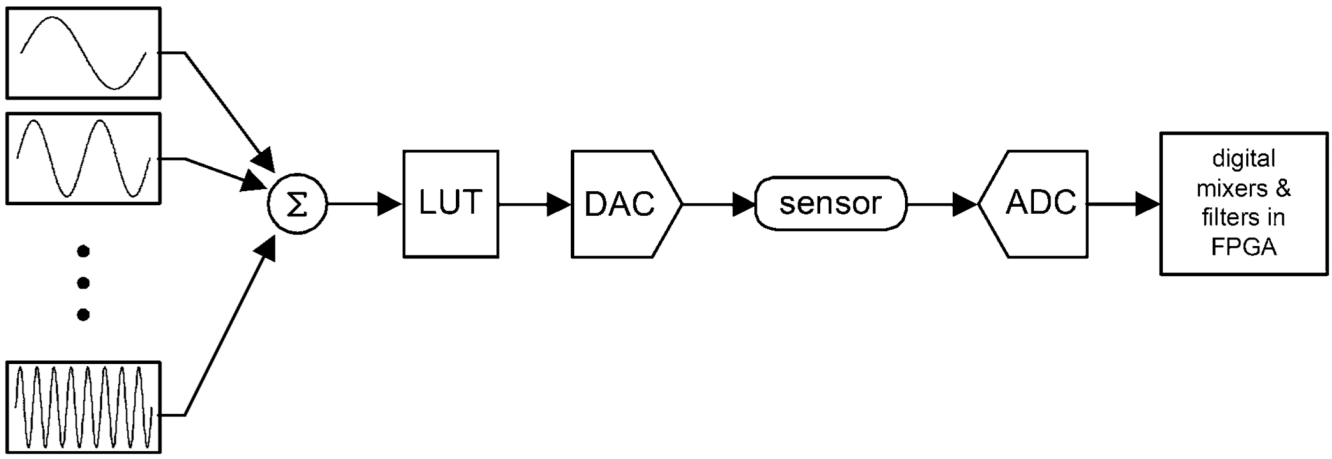

Fig. 12.

Scheme for ac impedance analysis of particles. AC electrical signals at several different frequencies are applied to sensing electrodes and the resultant signal is deconvoluted to reveal its real and imaginary components at the different frequencies. The desired frequencies are downloaded as a Fourier sum waveform to an arbitrary waveform generator. An ADC acquires the sensor response and this is decimated by an FPGA to derive in phase and out-of-phase frequency components.

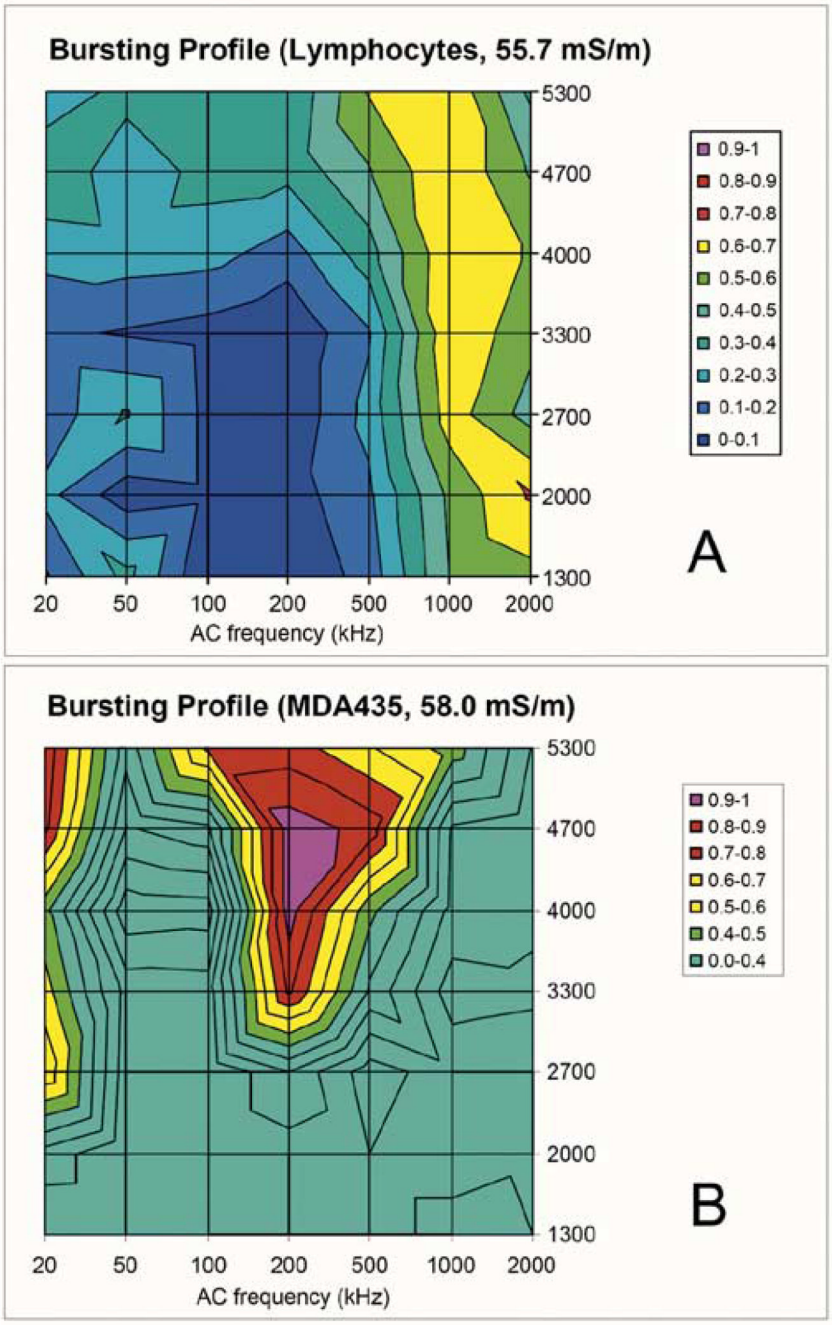

Fig. 13.
Electromediated bursting of cells. The fraction of cells destroyed is shown as a function of the applied field strength and frequency for: (a) T-lymphocytes and (b) MDA-MB-435 breast cancer cells.

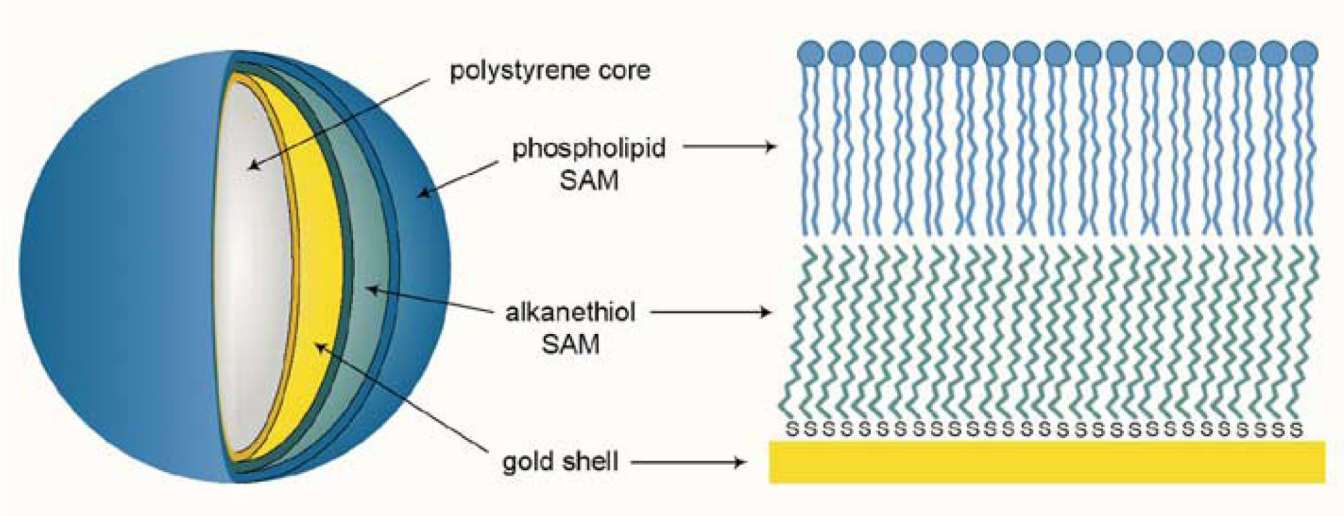

Fig. 14.

One type of engineered dielectric microsphere. The thickness of the insulating layer (and therefore, the dielectric properties) can be adjusted by changing the length of the hydrocarbon chains in the alkanethiol and phospholipid that are used to form the self-assembled monolayers.

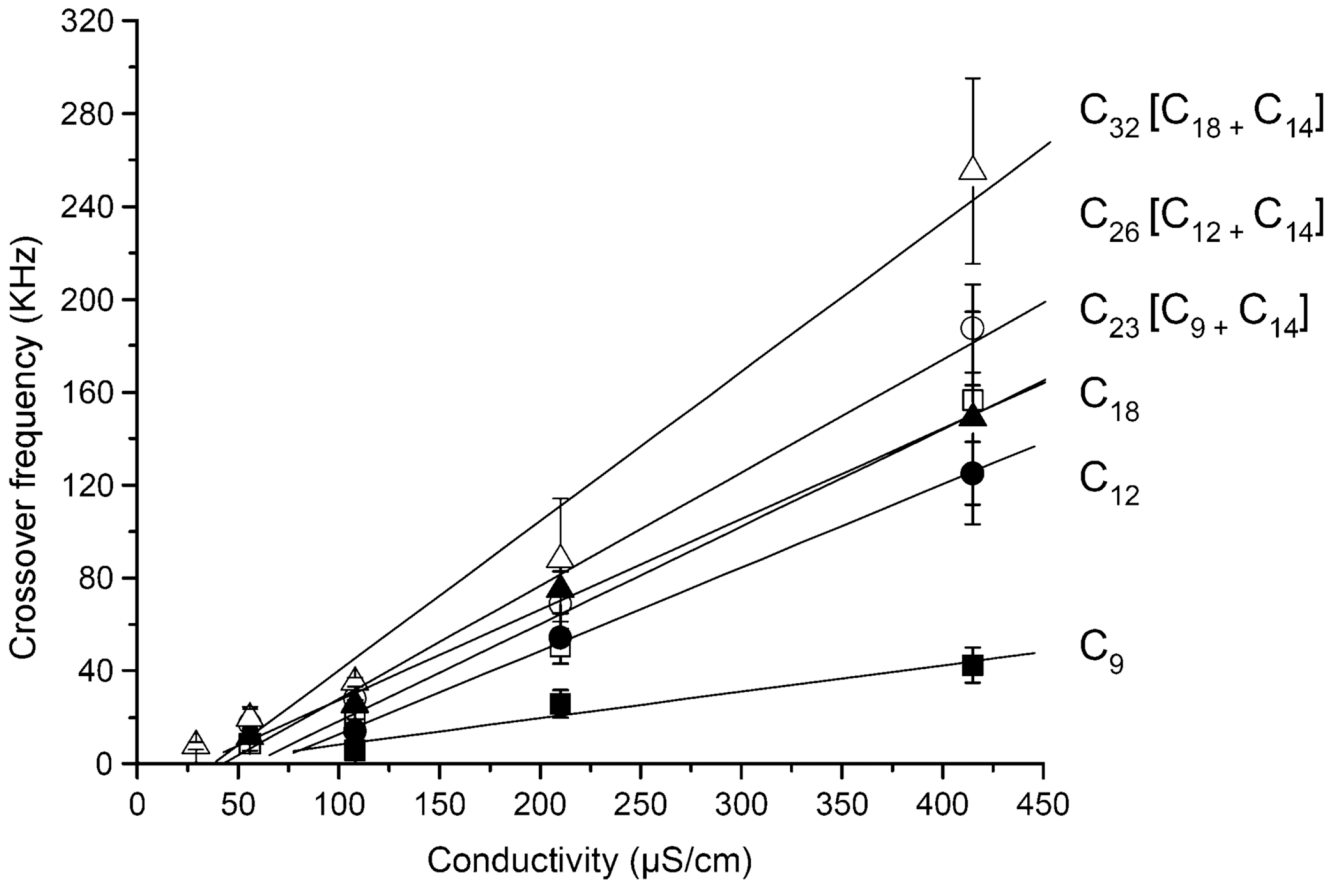

Fig. 15.
Dependence of DEP crossover frequency on insulating shell thickness for engineered dielectric microspheres.

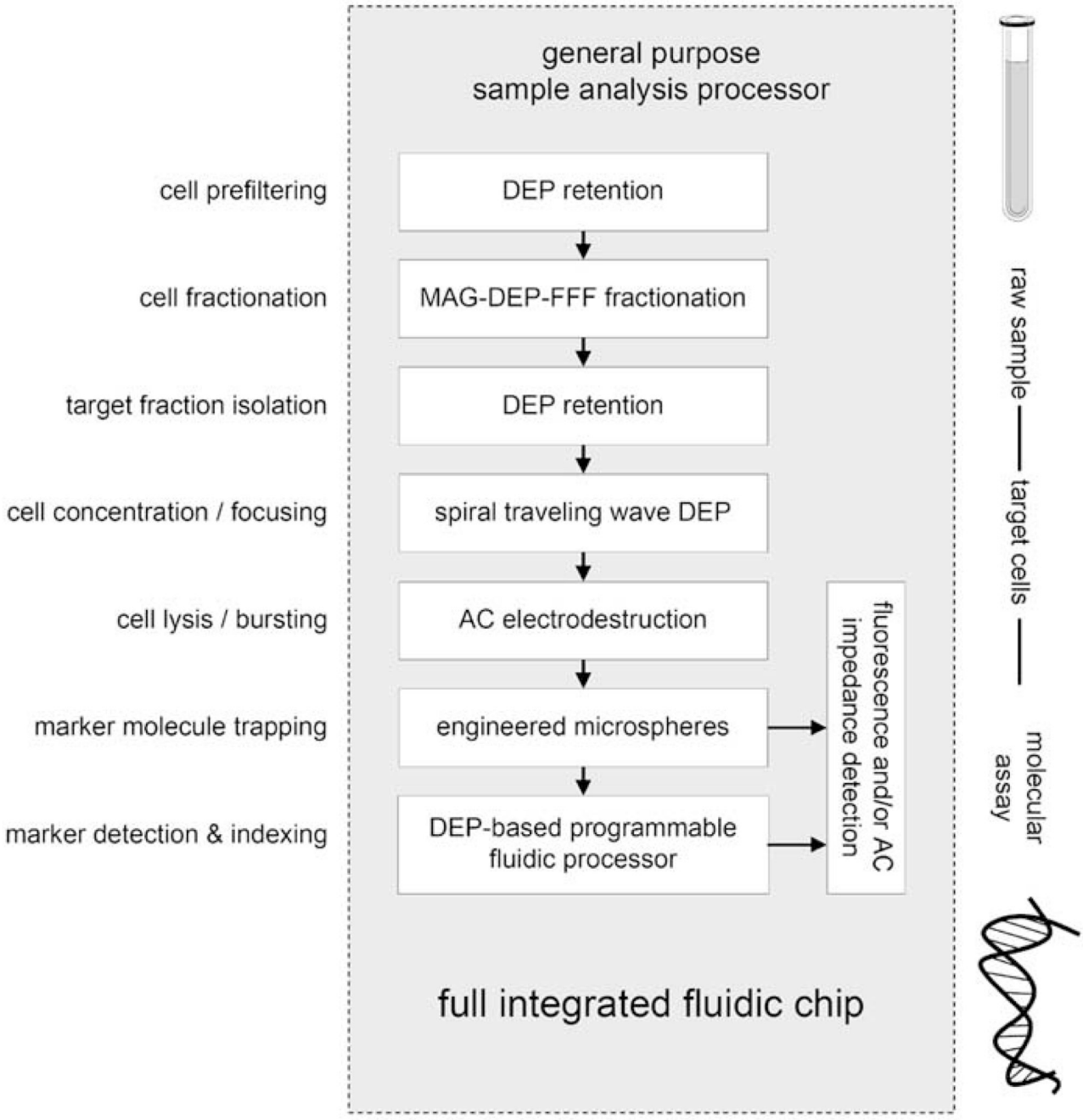

Fig. 16.
DEP-based technologies could be combined into a fully integrated micro total analysis system to perform all steps necessary for molecular diagnostics on a raw sample.